INTERNATIONAL WOOL TEXTILE ORGANISATION

TECHNOLOGY & STANDARDS COMMITTEE **NICE MEETING**

Commercial Technology Forum **December, 1998**

Chairman: D.J. WARD (Australia) **Report No: CTF 03**
Technical Coordinator: G. MERCIER (France)

Fundamental Principles of Fibre Fineness Measurement: the Airflow Instrument

By

P.J. Sommerville

Australian Wool Testing Authority Ltd, PO Box 190, Guildford, NSW 2161, Australia

SUMMARY

The Kozeny Equation has been the basis of all theoretical discussions of the various factors impacting upon the performance of the Airflow Instrument. In spite of this there has been very little information published which validates the predictions of the theory. The little that has been published suggests that the theory may not be a complete description of the physics of the instrument. The development of the theory is discussed, in the context of the development of the instrument itself. The results of a series of experiments designed to validate or invalidate the theory are also presented. These demonstrate that while the Kozeny Equation does correctly identify some factors that impact upon the Airflow Instrument, it does not provide a complete quantitative description of the effect of these factors. The reasons for this are discussed. In particular, the implications this may have for extrapolating calibration curves for the Airflow Instrument, obtained as described in IWTO-6 and IWTO-28, particularly for the measurement of fine and ultra-fine wool, are also discussed. Some observations are also made concerning the reported differences between LASERSCAN, OFDA and Airflow for ultra-fine wools.

INTRODUCTION

While newer technology such as Sirolan LASERSCAN and OFDA is gaining increasing favour, the Airflow is still the predominant instrument used for the determination of the fineness of wool fibre, in the greasy and in the semi-processed form. Measurements based on this instrument are still of major commercial importance, since fibre fineness is the most important factor in determining the market value of wool. The commercial trading of raw wool and semi-processed wool is still almost entirely based on fineness estimates provided by the Airflow instrument.

The development of our understanding of the physics of the Airflow instrument has been previously reviewed[1]. This review is briefly repeated here, but is expanded, to include additional material pertaining to the development of the Airflow Methods now in use. Furthermore, despite the general acceptance of the theory, there is little published information concerning its validation. What little information does exist is scattered among a number of publications. In this paper this information is for the first time summarised in a cohesive form.

In addition, some particular aspects of the theory have never been validated, at least for porous beds of wool fibre. Some simple experiments are reported which remedy this deficiency.

In developing the Airflow Method, and in attempting to maximise precision of the Method, the wool industry has to some extent been unaware of some implications stemming from the physics of the instrument. The consequences of this are becoming increasingly obvious now that the diversity of instrumental methods available for determining the mean diameter of wool fibre has increased. Sommerville[1], and Lindsay and Marler[2] have recently highlighted one of the consequences of this approach, by firstly validating the theory describing the effect of coefficient of variation in diameter[1], and then quantifying the magnitude of this effect in blends of wool tops[2]. There are also other consequences, and these are discussed in this paper.

NOTATION

The mathematical notation used throughout the following sections is summarised below. Unless considered absolutely necessary for clarification of the particular discussion, this notation is not redefined each time an equation is introduced or used. The same notation is used in many of the equations, and every effort has been made to ensure consistent usage of the symbols in relation to specific physical parameters. Differentiation, when required, has been achieved by using subscripts or superscripts.

The units and hence all calculations are in cgs units. One parameter where cgs units have not been used is the unit for fineness. The Wool Industry has adopted the term "micron" for this very important parameter. This is an abbreviation for the equivalent SI unit "micrometres". The term "fineness" and "diameter" are used interchangeably throughout the text. The other exception is pressure differences. These are generally expressed in mm, but in all calculations this is converted to the cgs unit, dynes cm^{-2}.

Q = Average flow (cm^3/sec).

k = Kozeny Constant.

g = Acceleration due to gravity (cm/sec^2).

h = Viscosity of air (dynes-cm/sec^2).

A_c = Cross-sectional area of the Airflow chamber (cm^2).

L_c = Depth of the Airflow chamber* (cm).

V_c = Volume of the Airflow chamber (cm^3).

ΔP = Pressure difference across the bed (g/cm^2).

e = $\frac{V_c - V_m}{V_c}$, porosity of the fibre mass.

V_m = Volume of the fibre mass (cm^3).

A_m = Surface area of the fibre mass (cm^2).

S = Surface area of a channel per unit volume of fluid filling the channel (cm^{-1}).

S_0 = Specific Surface (cm^{-1}).

d = Mean diameter of the fibres (microns).

$\bar{d}$ = Length proportioned mean diameter as determined by the projection microscope.

$\bar{d}^2$ = Length proportioned mean square diameter.

ℓ = Total length of the fibres (cm).

C = Fractional Coefficient of Variation in $\bar{d}$.

$$K = \frac{gA_c}{16khL_c} \cdot \frac{e^3}{(1-e)^2} \cdot \left(1 + C^2\right)^2$$

$$K_A = \frac{1}{Q} \cdot \frac{gA_c}{16khL_c} \cdot \frac{e^3}{(1-e)^2}$$

$$K_d = \frac{gA_c}{16khL_c} \cdot \frac{e^3}{(1-e)^2} \cdot \left(1 + C^2\right)^2$$

H = Airflow rotameter flow meter height (cm).

$$K_P = \frac{gA_c}{16khL_c} \cdot \frac{e^3}{(1-e)^2} \cdot \left(1 + C^2\right)^2 \bar{d}^2$$

$$K_e = \frac{gA_c}{16khL_c} \cdot \Delta P \cdot \left(1 + C^2\right)^2 \bar{d}^2$$

$$K_C = \frac{gA_c}{16khL_c} \cdot \Delta P \cdot \frac{e^3}{(1-e)^2} \cdot \bar{d}^2$$

$$K_{Cd} = \frac{gA_c}{16khL_c} \cdot \Delta P \cdot \frac{e^3}{(1-e)^2}$$

u = Face velocity of the gas (cm/sec).

G = Linear mass velocity (g/cm^2/sec).

r = Density of the gas (gm/cm^3).

r_S = Density of gas at standard conditions.

r_m = Density of the gas at the arithmetic mean pressure P_A .

P = Pressure of gas (dynes/cm^2).

P_S = Absolute pressure on the input side of the plug (assumed to be standard conditions).

P_1 = Absolute pressure on the output side of the plug.

$\Delta(P^2) = \left(P_S^2 - P_1^2\right)$ in $(gm/cm^2)^2$.

$P_A = \frac{(P_S + P_1)}{2}$, the arithmetic mean pressure.

Q_i = Input flow to the plug.

R = Universal gas constant, in absolute units.

T = Absolute temperature (degrees Kelvin).

M = Molecular weight of the gas.

k_0 = Modified Kozeny constant that allows for the tortuous path followed by the fluid as it flows through the bed (approximately equal to 2.5).

d = Variable factor (≈ 0.9).

Q_K = Flow predicted by Kozeny Equation.

R_H = Mean hydraulic radius (cm).

* Note that these dimensions are describing the dimensions of the fibre plug when compressed in the chamber

THE PHYSICS OF THE AIRFLOW INSTRUMENT

THEORETICAL PRINCIPLES

An earlier paper described the basis of the theoretical model used by wool technologists in describing the behaviour of the Airflow instrument[1]. This model was derived from a number of empirical and theoretical studies describing the flow of liquid and gaseous fluids through capillaries and porous beds. These occurred over a period of approximately 100 years, with individual contributions from Poiseuille (1840), Darcy[3], Dupuit (1863), Greenhill[4], Blake[5], Kozeny[6] and Carman[7,8]. Wiggins, Campbell and Maas[9] first applied this model to describe the flow of liquids through beds of fibres. Fowler and Hertel[10] studied the flow of air through plugs of cotton, wool, rayon and glass wool, and found substantial compliance with the predictions of the theory. Sullivan and Hertel[11], and Grimes[12] demonstrated the practical application of the theory in determining the Specific Surface or fineness of cotton fibres. Cassie[13] was the first to apply the principles of this model directly to the measurement of wool fineness, where the fibres were arranged in parallel array. Anderson and Warburton[14] refined this technique by demonstrating the benefit of ensuring a random orientation of the fibres in the fibre bed.

It was postulated that the flow of air through a compacted bed of randomly oriented wool fibres is described by the Kozeny Equation (see Equation 1).

$$Q = \frac{gA_c}{khL_c} \cdot \Delta P \cdot \frac{e^3}{(1-e)^2} \cdot \left(\frac{V_m}{A_m}\right)^2 \qquad (1)$$

Carman[8] introduced the concept of Specific Surface, S_o, described as follows by Equation 2.

$$S_o = \frac{A_m}{V_m} \qquad (2)$$

By substituting Equation 2 into Equation 1, the Kozeny Equation assumes the form:

$$Q = \frac{gA_c}{khL_c} \cdot \Delta P \cdot \frac{e^3}{(1-e)^2} \cdot \frac{1}{S_o^2} \qquad (3)$$

Cassie[13] assumed that the fibres were circular in cross-section, and hence the Specific Surface could then be defined in terms of the mean diameter. Neglecting the areas at the end of the fibres, the surface area then becomes $p d \ell$, where ℓ is the length, and the volume is $p d^2 \ell / 4$; or

$$S_o = \frac{4p}{p} \cdot \frac{d\ell}{d^2 \ell} = \frac{4}{d} \qquad (4)$$

Hence it follows that:

$$Q = \frac{gA_c}{16khL_c} \cdot \Delta P \cdot \frac{e^3}{(1-e)^2} \cdot d^2 \qquad (5)$$

Anderson and Warburton[14] pointed out that the fineness of wool fibre is variable between fibres and along fibres, and accordingly, the approximation of **uniform** circularity implied by Equation 4, is too simplistic. More rigorously:

$$S_o = \frac{\int 4p d \cdot d\ell}{\int p d^2 \cdot d\ell} \qquad (6)$$

where the integrals are then over the total length of the fibre in the plug. It can be shown that

$$S_o = 4 \cdot \frac{\bar{d}}{\bar{d}^2} \qquad (6a)$$

where $\bar{d}$ is the length proportioned mean diameter as determined by the projection microscope (note that this still assumes circularity of cross-section) and $\bar{d}^2$ is the similarly proportioned mean square diameter. Anderson and Warburton[14] then demonstrated the familiar relationship:

$$d = \bar{d}\left(1 + C^2\right) \qquad (7)$$

Therefore, Equation 5 is more correctly expressed as follows:

$$Q = \frac{gA_c}{16khL_c} \cdot \Delta P \cdot \frac{e^3}{(1-e)^2} \left(1 + C^2\right)^2 \cdot \bar{d}^2 \qquad (8)$$

Some obvious implications can be drawn from Equation 8. Imagine that a mass of wool fibres, where the fibres are randomly oriented with respect to each other, is compressed in a chamber of fixed dimensions. Further, imagine that the chamber has a porous base and top, which offer no significant resistance to the flow of air through the chamber. Then, the flow of air through the chamber will be determined by the pressure difference, the porosity, the coefficient of variation in fibre diameter and the mean length proportioned diameter. Essentially, this is a description of the modern Airflow instrument (see Figure 1 on the following page).

APPLICATION OF THE THEORY

The development of sample preparation techniques is as much a part of the development of the Airflow Method as the development of the instrument. However, this is a sufficiently broad subject to warrant separate consideration. Consequently, sample preparation will not be discussed here.

The early development of the Airflow instrument was based on the observation by Anderson and Warburton[14] that the effect of C, the Coefficient of Variation in Diameter, ***in the case of wool tops***, was very small, and certainly less than the errors arising from other sources of variation. Consequently, it was assumed that the physical behaviour of the instrument is adequately described by Equation 5. By ensuring constant porosity, constant pressure) were described by Anderson[15] in 1954, together with procedures for preparing the samples, calibrating the instruments with tops (where the mean diameter had been determined by Projection Microscope), and conducting the measurements. It is of interest that Anderson clearly inferred that the calibration curve for the Version A instrument was non-linear, while the calibration curve for the Version B instrument was approximately linear. The form of Equation 9 suggests that both curves should be non-linear.

In 1954 Monfort[16] provided the first report of the industrial application of the Airflow instrument. "*We have examined Anderson's apparatus (Version A) and seen this used in industrial conditions. It has given entirely satisfactory service and it has replaced the*

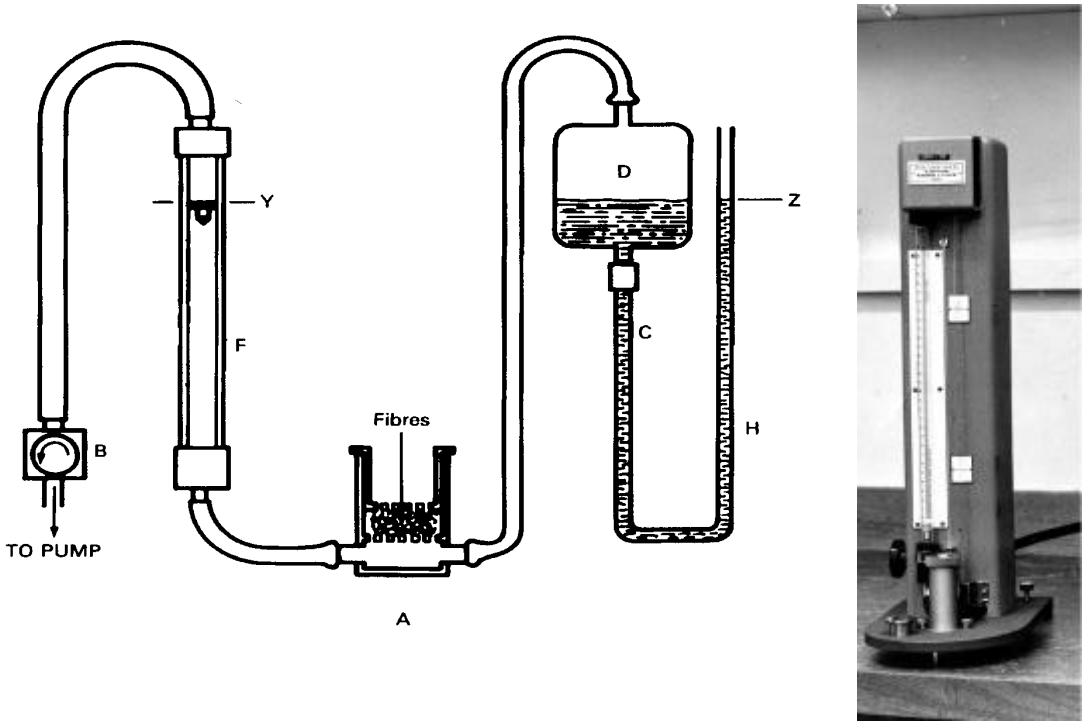

Figure 1: The design of the constant pressure, variable flow Airflow apparatus used in IWTO-6 and IWTO-28 was developed by WIRA. Most of the early development work was conducted using the variable pressure, constant flow instrument. However the fundamental principles on which both instruments are based are the same. This illustration shows the operation of the instrument in a schematic form. The apparatus consists of a constant volume chamber (A), a manometer (H) connected by a tube (C) to a fluid reservoir (D), a flow control valve (B) connected to a vacuum pump, and to a flow meter (F). The plug of wool fibres is placed in the chamber A and compressed to a constant volume by a perforated plunger. The valve B is opened until the flow is stable and the manometer liquid level is stabilised at a constant point Z. The height (Y) of the rotameter flow meter (F) is then recorded.

Equation 5 reduces to

$$Q = K \cdot \Delta P \cdot \bar{d}^{2} \qquad (9)$$

Therefore, two designs of the instrument are possible:

- Constant flow and variable pressure
- Variable flow and constant pressure.

Two such instruments, Version A (constant flow, variable pressure) and Version B (variable flow and *lanometer for 90% of the fineness measurements by Pelzer and Fils*." The calibration of the instrument assumed the function:

$$K_A = \Delta P \cdot \bar{d}^{2} \qquad (10)$$

where K_A was assumed to be constant.

Clearly this is simply another way of expressing Equation 9 in the case where the flow is maintained

constant. A linear expression of Equation 10 can be obtained by a logarithmic transformation:

$$\log \Delta P = -2 \log \bar{d} + \log K_A \qquad (11)$$

The International Wool Textile Organisation's (IWTO) standard methods for fineness measurement by Airflow are based on the Version B instrument[17,18], although IWTO-6 also includes Version A. If the theory is correct, then the appropriate calibration function for the Version B instrument should be of the form:

$$Q = K_d \cdot \bar{d}^2 \qquad (12)$$

where K_d is constant. The logarithmic transformation in this case takes the form:

$$\log Q = 2 \log \bar{d} + \log K_d \qquad (13)$$

However, in both IWTO standards, the required calibration function takes the form:

$$Q = a + b \cdot \bar{d} + c \cdot \bar{d}^2 \qquad (14)$$

where a, b and c are constants. This is a quadratic function, which is derived purely on a statistical basis. In practice, the value of c is very small, and consequently, Equation 14 describes a almost linear relationship between flow and mean diameter, over the range of fibre diameter encompassed by the calibration material (see Figure 2).

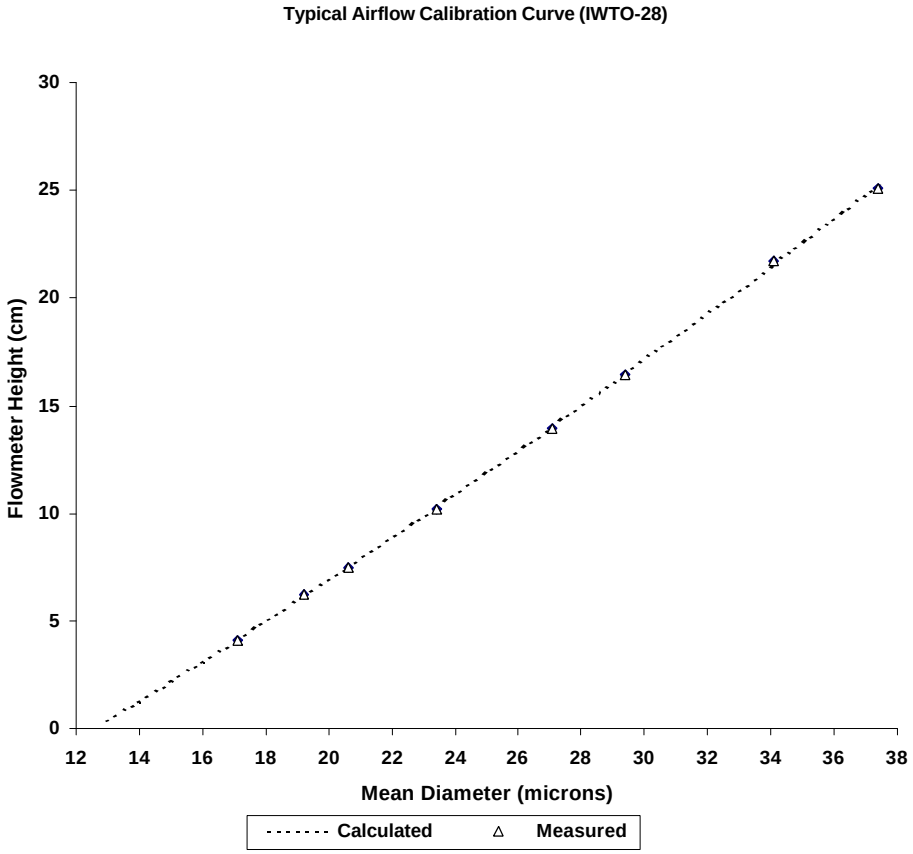

Figure 2: This is an example of a typical calibration curve for a constant pressure variable flow Airflow instrument. The actual calibration points are shown, overlayed by the regression equation that has been fitted to the points by the procedures defined in IWTO-28 i.e.

$$H = 10.4412 + 0.7676\bar{d} + 0.00496\bar{d}^2$$

This has been extrapolated to 13 microns. Note that the curve is very nearly linear, and therefore, it seems reasonable to expect that extrapolation errors should be small and the measurement limited only by the range of the flow meter.

Mann[19] drew attention to this in 1970, and argued that the regression Equation in the IWTO Standards should assume a linear model, there being little improvement in the regression by assuming a quadratic model. Anderson and Settle[20] claimed that a logarithmic function would be more appropriate than the quadratic expression in the IWTO Standards. "*With regard to the relation between flow meter reading and fibre diameter, we conducted an intensive search for the function that gives the best transformation to a linear relation. We have found that a plot of the logarithm of flow against*

the logarithm of the published value of fibre diameter gives the highest correlation of all those tried."

$$\log Q = 1.97 \log \bar{d} + constant \qquad (15)$$

Equation 15 is an example of the relationship that these authors derived from their calibration data. Note that it is virtually identical to Equation 13, the relationship the theory predicts. Anderson had already presented this view to IWTO in 1963[21] but the recommendation had not been accepted.

James[22] responded to these remarks. "*The letters of Mann and Anderson and Settle have missed an important point. There is no direct relationship between the theoretical relationship quoted by Mann and the quadratic curve-fitting equation specified by the IWTO. It is agreed that there is this theoretical basis for the dependence of airflow on diameter, but the actual airflow is not the subject of the IWTO calibration. The IWTO calibration relates the height of the float in the rotameter flow meter to diameter. The rotameters are manufactured with a quadratic relation between the height of float and airflow. Because the IWTO calibration uses flow meter float height, there is no theoretical reason for expecting this to vary as the square of the diameter, even if flow does so.*"

This argument is misleading, and Anderson[23] quickly pointed this out. The rotameter flow meter is not manufactured such that there is a quadratic relation between the height of the float and the airflow. However, individual flow meters manufactured at that time did exhibit small deviations from linearity, such that the flow versus height relationship could be **more accurately** represented by a quadratic expression of the type

$$Q = a + b \cdot H + c \cdot H^2 \qquad (16)$$

The coefficient of the squared term was very small and regressions based on Equation 16 were very nearly linear. Anderson[23] also observed that "*the constant-flow type of air-flow instrument does not require any intermediate flow meter calibration, since only one position of the float is used. Furthermore, the heights of the manometer menisci above a datum point may be considered to be fundamental units of pressure (apart from variations in barometer). This was realised at the time, and, in fact, this type was the laboratory prototype of the airflow method. However, it was reluctantly decided that the very marked non-linearity of the scale made it much less acceptable to industry, so the constant-pressure type was chosen as the commercial instrument.*"

The non-linearity of the Airflow calibration function has also been criticised by Baxter, Brims and Taylor[24]. These authors quite correctly recognised that a non-linear calibration function placed limitations on the accuracy of the calibration function, when extrapolating outside the range of diameters provided by the calibration samples. However, this limitation has not been of any real significance until recent years. The availability of rapid and relatively inexpensive tests for mean fibre diameter, based on the new technology that has emerged, has assisted the production of commercial quantities of ultra fine wool[25], with a mean diameter well outside the range of the calibration standards.

The reason why the calibration of the constant-pressure instrument is very nearly linear, when the theory suggests it should be curvilinear has never been adequately explained. Until the past few years, this has never really been an issue of importance. The thrust of the earlier work was to develop a low cost method with maximum precision, and for this reason the calibration function was selected, to provide the optimum fit to the experimental data, rather than satisfying any particular theoretical model.

EXPERIMENTAL VALIDATION

In principle the experimental validation of this model is relatively simple. Due to the design of the Airflow instrument, and the definition of the measurement environment, the first ratio in Equation 8 should be constant. Hence:

$$Q = function\left(\Delta P, e, C, \bar{d}\right) \qquad (17)$$

In the case where e, C and $\bar{d}$ are maintained constant, then the effect of pressure is defined by:

$$Q = K_P \cdot \Delta P \qquad (18)$$

Likewise, when ΔP, C and $\bar{d}$ are maintained constant, then the effect of porosity is defined by:

$$Q = K_e \cdot \frac{e^3}{(1-e)^2} \qquad (19)$$

Furthermore, when ΔP, e and $\bar{d}$ are maintained constant, then the effect of coefficient of variation of fibre diameter is defined by:

$$Q = K_C \cdot \left(1 + C^2\right)^2 \qquad (20)$$

Finally, in the case where ΔP, e and C are maintained constant, then the effect of diameter is defined by:

$$Q = K_d \cdot \bar{d}^2 \qquad (21)$$

Provided the necessary conditions are satisfied, plots of the variables in Equations 18, 19, 20 and 21 should be linear, with constant slopes of K_P, K_e, K_c and K_d respectively. If suitably designed experiments confirm this expectation then the model can be considered validated.

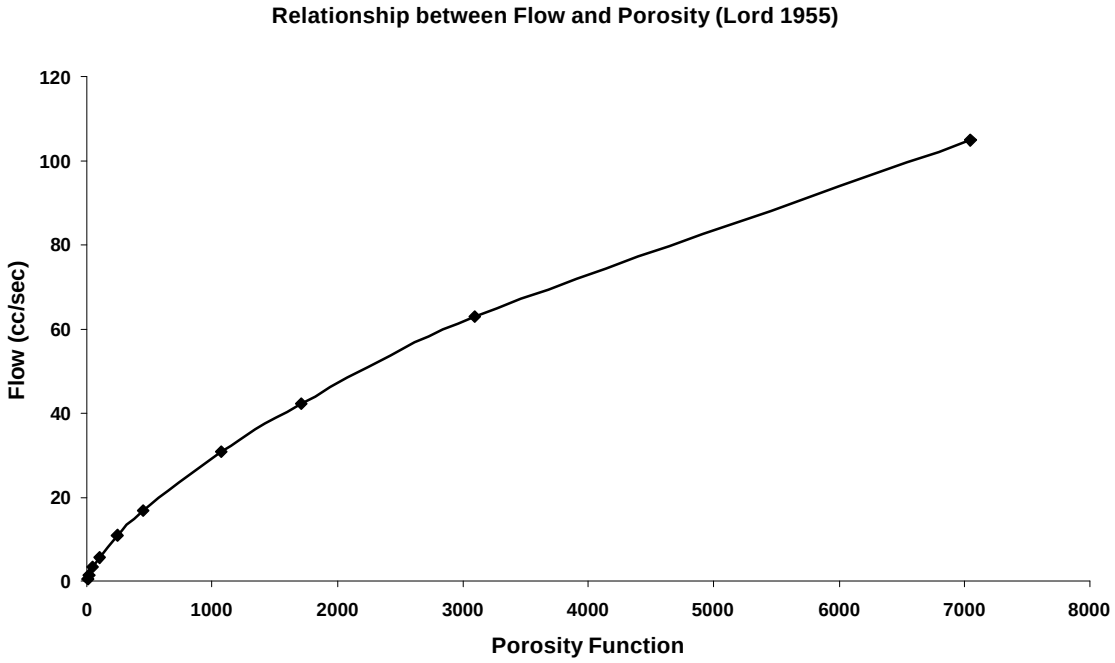

Figure 3: The theoretical curve for the relationship between the flow and the porosity function is linear, as described by Equation 19. However, the data reported by Lord[28] suggests that this is not the case. In this graph Lord's data for a wool top is plotted using Equation 19. Quite clearly, the relationship is not linear.

Despite the apparent simplicity, there have been very few reports in the relevant literature of any experiments specifically designed for this purpose. In hindsight this does seem a little strange, since the theory is frequently quoted. It is only recently that Sommerville[26] and Lindsay and Marler[27] have published data confirming effects predicted by Equation 20. However, the emphasis of the technologists at the time was to develop a rapid and reliable instrument for the estimation of mean fibre fineness, as a replacement for the relatively inefficient gravimetric and optical projector methods that were the only other means available. Whether or not the theoretical model used to explain the observed effects is actually valid was probably of secondary importance.

The cotton industry had shown a little more interest in the basic physics. However, this was to some extent out of necessity rather than more substantive technical insight. Unlike wool, cotton does not have an approximately circular cross section (except for very immature fibre) and consequently the best estimate of fibre fineness in this instance is an estimate of specific surface. Deriving the specific surface from airflow through plugs of cotton fibre necessarily involved a more direct application of the theoretical principles (refer to Equation 3).

In their original work, Anderson and Warburton[14] did note that the Kozeny Constant appeared to be diameter dependent. They included an empirical term in their equation for calculating the mean diameter from the flow, pressure and dimensional characteristics of their original instrument to compensate for this effect.

Lord[28] published the first systematic set of experiments that demonstrated the relationship between theory and practice. His primary interest was in cotton, but his paper also incorporated some limited information about wool.

Lord[28] was able to demonstrate that Darcy's Equation[3] applied to porous beds of randomly oriented cotton fibre. Under conditions of constant porosity, the flow was directly proportional to the pressure difference across the plug and inversely proportional to the length of the plug. Equation 18 is a simplified form of Darcy's Equation.

However, Lord[28] also reported porosity did not affect the airflow as predicted by the theory, and this observation applied to wool as well as a range of other fibres, including cotton. He estimated the Kozeny constant k as a function of porosity e, under conditions of constant pressure, and found that k was not in fact constant as e varied. As the porosity approached 1.0, k rapidly increased. His data, for wool top, is reproduced in a slightly different way in Figure 3. The data is plotted using Equation 19. If Equation 19 correctly describes the relationship between flow and porosity then the curve in Figure 3 should be linear. Clearly it is not, except for very high values of the porosity function, $e^3/(1-e)^2$.

Lord[28] conducted his experiments under somewhat different conditions from those for which the Airflow is designed to operate. He used quite low pressure differences (about 3 mm of water), in order to avoid the necessity to make any corrections to the flow arising from expansion of the air as it passed through the fibre plug. The Airflow instrument uses a constant pressure difference of about 180-mm.

To explain the aberrant behaviour that he observed, Lord[28] proposed a modification to the porosity term in the Kozeny Equation, such that Equation 3 becomes:

$$Q = \frac{gA_c}{khL_c} \cdot \Delta P \cdot \frac{e^5}{(1-e)^a} \cdot \frac{1}{S_o^2} \qquad (22)$$

where a is a fibre specific constant†. For the wool samples used, a = 1.253. However, this solution was completely empirical, without any theoretical basis. Lord suggested this empirical adjustment on the basis of measurements derived from a single wool sample, and samples of cuprammonium rayon, silk, cotton and viscose rayon. The measurements were conducted for only one pressure difference.

Lord[28] also cited a theoretical treatment by Emersleben[29], who examined a model describing flow along a system of parallel circular rods, equally spaced such that the centres of section fell on points of intersection of a square lattice. Emersleben[29] was able to show that for such a system, Darcy's law should apply. Lord[28] showed that this theory could be extended to explain the variation of k with e that he had observed, but he was unable to verify this observation quantitatively.

Richards (1954)[30] commented that *"it may easily be verified that flow is linearly related to pressure over the whole range, and a given percentage change in pressure produces the same change in flow."* She further commented as follows. *"There is evidence that, when fibres are comparatively widely spread, their resistance to fluid flow is more nearly described in terms of the aerodynamic resistance of a number of circular cylinders. This and possibly changes in density caused by medullation for coarse fibres lead to a nearly linear relation between air flow and fibre diameter, which is not expected from the Kozeny Equation."* Superficially this seems to confirm Lord's[28] observations regarding Darcy's Equation, but Richards[30] supplied no supporting data.

Neelakantan and Radhakrishnan[31,32] reviewed Lord's data in 1990. They found that "*the data do not conform to the formulas for air flow through fibre plugs as developed by Lord himself. The data can be better fitted by a family of three-parameter equations, but it is difficult to relate these parameters to the physical properties of fibres, such as linear density, form factor, and specific volume*". These authors suggested a set of empirically derived regression equations to better describe the data. However such simplistic approaches need to be treated with caution. Empirical models only retain their validity for the data from which they are derived, and unless the model has some theoretical basis it is most likely that it will fail when extended to new data.

Swan[33] has challenged the relevance of the Kozeny for describing the flow of air through a compressed bed of fibres. He pointed out that "*it is the reliance of the conventional models on Poiseuille's law for laminar flow through capillary tubes which leads to the postulated dependence of the rate of Airflow on the square of the fibre diameter*". He argued that the Kozeny model, which relies on the assumption that the pores in the bed can be represented as a series of parallel capillaries, is flawed. The "holes" or "pores" or "capillaries" in a fibre plug are not discrete (all interconnect), and the constituents of the fibre plug are more or less disarranged. Swan postulated that the mean free path of the air molecules passing through the plug is the dominant influence on the airflow. If the pores are small and convoluted, then the air molecules will frequently strike the fibres present, losing velocity and energy with each contact. This will translate to a large amount of energy expended in traversing the plug and hence the pressure drops across the plug. The greatest resistance to flow will be found in a fibre plug where the mean free path of the air molecules is least.

Swan[33] has not developed this model further. However, on the surface it does appear to assume that flow through the plug is turbulent rather than streamlined. Given the relatively low flow rates at which the Airflow operates, this assumption seems to be at odds with calculations of the Reynold's number for the system. These indicate that the flow is seriously laminar.

† The porosity term in this equation is reproduced as published by Lord. It was based on the observation that logarithmic plots of the variables ke^2 and $1/(1-e)$ were substantially linear for each type of fibre he considered. The lines through each set of plotted points appeared to radiate from a focus in the axis of $\log_{10} ke^2$.

METHODS AND MATERIALS

The 12th series of Interwoollabs calibration tops were used for this experiment. Samples of the tops were prepared and conditioned as described in IWTO-28.

A single WIRA Airflow instrument was used for all measurements.

The range of measurements that can be conducted on the Airflow instrument is limited by the design of the instrument. This range was extended in two ways. Firstly, a 30-cm rule was attached to the instrument to facilitate the recording of the manometer reading. This provided the ability to estimate the pressure drop to a resolution of 1 mm, over a range of 300 mm. Secondly a Model 8350 VELOCICALC Air Velocity Meter (manufactured by TSI Incorporated[34]) was used to measure the airflow, in conjunction with the rotameter on the Airflow instrument. The VELOCICALC actually records air velocity. The measurement technique used is constant-temperature hot-wire anemometry in which the sensor is held at a constant temperature by a control circuit. As the speed of the air flowing past the sensor increases, more electrical power is required to maintain the sensor's temperature. Thus the power supplied to the sensor is directly proportional to the air velocity. The instrument is provided with a calibration certificate and has an average accuracy over its range of ±0.15 %.

A special fitting was manufactured to house the sensor of the TGI instrument, so that the cross-sectional area of the air flow stream passing over the sensor was accurately known. The fitting could be locked down onto the top of the plunger once the plunger was inserted into Airflow instrument chamber. Thus the instrument could be used to record the velocity of the air flowing into the chamber, and by multiplying this velocity by the area of the aperture in which the sensor was mounted, the volume flow was calculated.

The VELOCICALC instrument was also used to calibrate the rotameter, under conditions where the pressure difference across the chamber was zero. This was achieved by placing the plunger in the chamber. By progressively opening the valve on the Airflow instrument, thereby increasing the flow through the chamber, the VELOCICALC readings corresponding to 20-mm intervals on the Airflow rotameter were recorded.

A series of measurements was made using each of the IH tops and a range of plug weights for each top. The plug weights ranged from 1.250 grams to 3.000 grams, with an interval of 0.250 grams between the weights. This provided a maximum of 9 separate plug weights, although in practice the full range could only be used for the finest top. As the mean fibre diameter increased, measurements for the lower plug weights became increasingly impracticable.

Each weighed plug was placed in the chamber, the plunger inserted, and the air velocity sensor fitting placed over the plunger. The entire assembly was then locked down so that the fibre mass was fully compressed to the standard volume. Two series of measurements were recorded for each plug weight for each top. Firstly, the pressure difference was adjusted to a constant value, and the air velocity entering the plug was recorded. Where possible, the corresponding rotameter reading was also recorded. These readings were conducted at intervals of 20 mm of pressure over the full 300-mm range, giving 16 readings in total. Secondly, the flow was adjusted to a constant value, using the rotameter. The corresponding air velocity and manometer height was then recorded. These readings were also conducted at intervals of 20-mm on the rotameter, over the full 300-mm range.

The calibration of the rotameter with the air velocity meter was repeated after a complete set of readings had been obtained for all plugs for each particular calibration sample.

EXPERIMENTAL RESULTS

The measurements recorded from the VELOCICALC instrument, for the constant pressure series of measurements, form the most comprehensive set of data for all the variables involved in this experiment, and will be used for most of the data analysis. These are shown in Appendix A, Tables A1, A2, A3 and A4. These data represent separate experiments conducted some months apart. The air velocity measurements from the VELOCICALC meter have been converted to volume flows (cm^3/sec) by multiplying the recorded air velocities by the aperture area of the mounting for the VELOCICALC sensor. The small differences in the flow data for equivalent experimental conditions are partly due to a different plunger being used in each experiment.

The flow data in Tables A3 and A4 were obtained at the same time as the data in Table A2. These additional samples were fleece wools chosen to extend the range of diameters further into the ultra-fine region. The fineness of these samples was determined using both OFDA and Sirolan LASERSCAN.

CALIBRATION OF THE ROTAMETER

The experiment provided two sets of information for calibrating the rotameter on the Airflow, using the air velocity data.

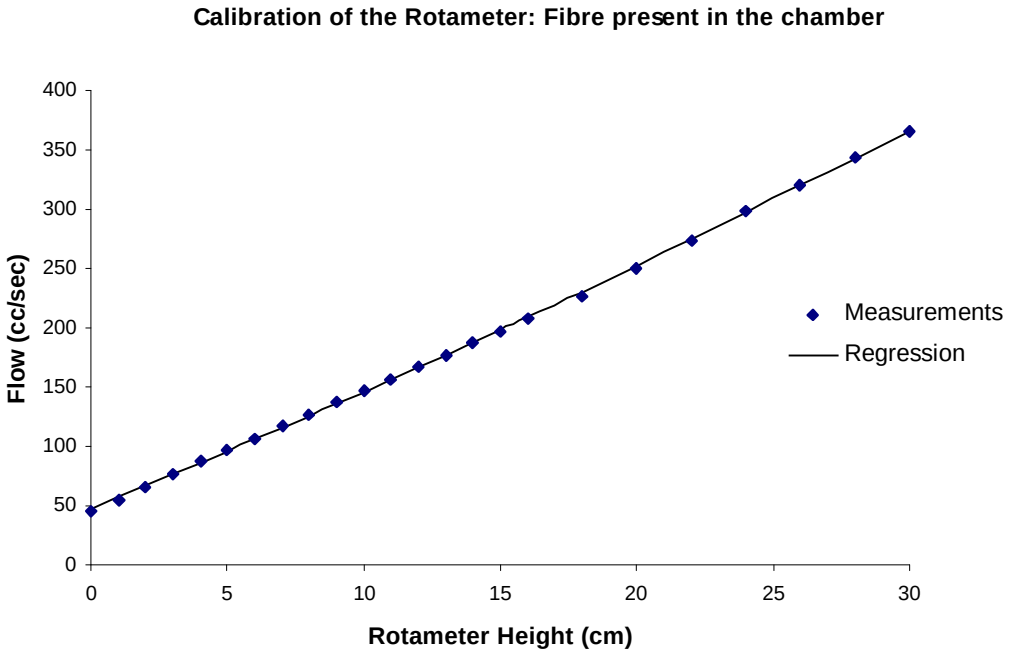

Figure 4: The above chart shows the relationship between the air flow measured using the VELOCICALC instrument and the height of the Airflow rotameter. The data points are averages, based on all the readings made when the flow was held constant, for the range of plug weights and mean fibre diameters. As expected, the relationship is independent of plug weight or of mean fibre diameter. The solid line is the line of best fit based on a quadratic regression:

$$Q = 47.61 + 9.45H + 0.0386H^2$$

This relationship has the same form as reported by James, and reflects the slight deviation from linearity over the length of the rotameter reported elsewhere.

The calibrations conducted without any fibre in the Airflow chamber provided one set. The data obtained from the series of measurements where the flow was adjusted to a constant value, using the rotameter, and the corresponding air velocities and manometer heights were recorded, provided a second set. The calibration curve derived from this second set of data is shown in Figure 4. The reason for calibrating the rotameter was to enable these data to be used to verify any trends observed in the VELOCICALC data. However, the range of data points that can be used from the rotameter was somewhat smaller than for the VELOCICALC for obvious reasons. In particular, the rotameter was useless for recording flows less than approximately 50 cm^3/sec (see Figure 4). The rotameter values were also used to check the stability of the electronic flow meter over the duration of the experiments.

INFLUENCE OF PRESSURE ON AIR FLOW

Table A1 includes a considerable amount of data that can be used to examine the relationship between pressure and flow. The data set for the 16.66 micron top is the most extensive and this has been used to construct Figure 5 (see next page). This figure shows a plot of flow versus pressure for this top, and for a number of different plug masses (a lower plug mass corresponds to a higher porosity).

It is immediately apparent, that while the relationship is very nearly linear over the range of plug masses used, it is still slightly curvilinear, with the curvilinearity decreasing as the pressure difference approaches zero. Linear regressions have been fitted to the linear portions of these data, and these are shown in Figure 5 (see next page) as dashed lines. The values of the relevant statistics are summarised in Table 1. When the regression lines are extrapolated, they converge to a narrow region on the x-axis, at a negative value. This suggests that the factor responsible for the curvilinearity is consistent over the range of the fibre mass and pressure used, and must be varying systematically with the pressure difference. These data suggest that Equation 18 is an incomplete description of the relationship between flow and pressure difference. A linear relationship is predicted by Darcy's Law, and has been experimentally verified for other fibres and for powders. It does not appear to be the case in this instance over the full range of pressure differences.

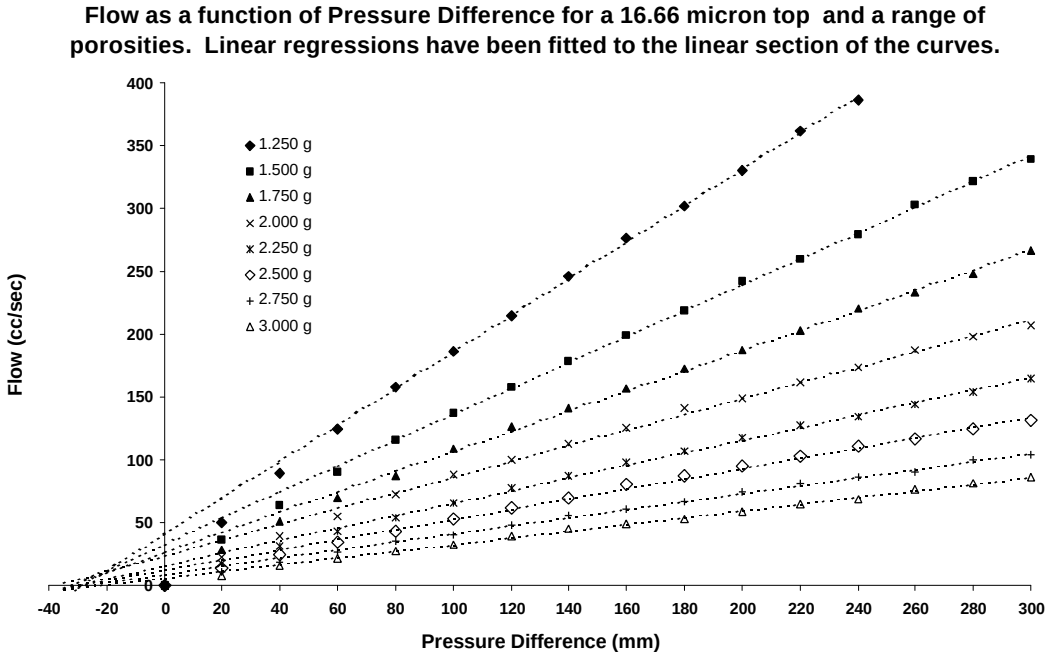

Figure 5: The flow rate as measured by the VELOCICALC is plotted as a function of pressure difference for a 16.66 micron top and for plug weights ranging from 1.250g to 3.000 g. Note that the resultant points do not lie on a straight line as expected from Equation 18. However, above a pressure difference of 50 - 100 mm the points appear to be approximately linear. Linear regressions have been fitted to the points corresponding to pressure differences greater than or equal to 80 mm.

Table 1: Summary statistics for linear regressions fitted to Flow vs Pressure data

	Plug Mass (g)							
Statistic	1.250	1.500	1.750	2.000	2.250	2.500	2.750	3.000
R Square	0.9995	0.9994	0.9983	0.9966	0.9978	0.9967	0.9973	0.9986
Intercept	40.69	32.84	26.61	23.72	15.98	12.40	9.31	6.19
Std Error	1.83	1.73	1.93	2.12	1.37	1.35	0.97	0.58
Slope	1.45	1.03	0.80	0.63	0.50	0.41	0.32	0.27
Std Error	0.01	0.01	0.01	0.01	0.01	0.01	0.01	0.00

INFLUENCE OF POROSITY ON AIR FLOW

Figure 6 (see next page) plots flow as a function of $e^3/(1-e)^2$, for a range of pressure differences. Once again, the diameter of the wool top used to obtain these data was 16.66 microns. Equation 19 predicts that this relationship should be linear. Clearly it is not. The data is very similar to that reported by Lord (see Figure 3) although the values of the porosity function are very much lower in this instance. However, the curvilinearity does become more pronounced as the pressure difference increases. Conversely the curves become more linear as the porosity function increases. This suggests that extrapolating the linear portions of these curves will result in the lines converging on narrow area on the x-axis in exactly the same way as they do in Figure 5. Regression lines have been fitted to the linear portions of the curves and confirm this is the case.

As previously this suggests that the factor responsible for the curvilinearity is consistent over the range of the measurements, but in this case must be varying systematically with the porosity. These data suggest Equation 19 is also an incomplete description of the relationship between flow and porosity.

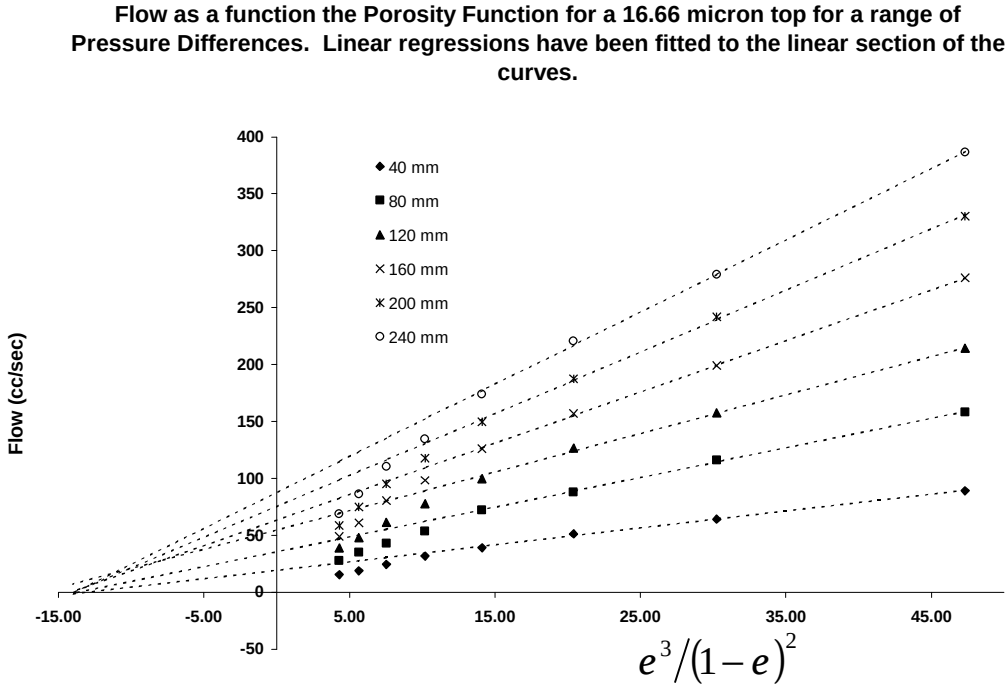

Figure 6: This graph shows the flow plotted as a function of the porosity function $e^3/(1-e)^2$, for a range of pressure differences. A 16.66 micron top has been used. The relationship is clearly curvilinear and is very similar to that reported by Lord[28], except that he used a much coarser top. Regression lines have been fitted to the linear portions of the curves (corresponding to values of the porosity function greater than or equal to 15.00) and extrapolated to intersect with the horizontal axis, in the same manner as in Figure 5. In this case also, the lines converge to a narrow area on the horizontal axis

FLOW AND COEFFICIENT OF VARIATION

Top samples with characteristics suitable to demonstrate the validity of Equations 20 and 21 do not exist. However, Sommerville[1] created fibre blends with the same mean fibre diameter[‡] (25.0 microns) but with substantially different coefficients of variation in mean fibre diameter, and measured these blends using Sirolan LASERSCAN, OFDA and Airflow. These data can be used to test whether the relationship between flow and coefficient of variation in fibre diameter is adequately described by Equation 20.

Sommerville[1] demonstrated that within the range of Coefficient of Variation in Diameter encompassed by his data, the relationship between fineness as defined by Airflow, Coefficient of Variation in Diameter and fineness as defined by the Projection Microscope is at least approximately described by Equation 7. Using the data in Table A1, these Airflow data have been converted to equivalent flows and Figure 7 (next page) shows the relationship described by Equation 20 derived from this transformation. For the range of data available the relationship appears to be linear. However, no data exists for values of $(1+C^2)^2$ in the range 1 to 1.15, and consequently, whether or not the curvilinearity observed in Figures 5 and 6 exists in this case also, cannot be determined.

Note that the term on the x-axis of Figure 7 can never be less than unity. Hence the point at which the extrapolation of the regression line cuts the y-axis represents the flow through a plug where each fibre has a uniform diameter of 25 microns. From the appropriate form of the Kozeny Equation represented by Equation 5 it is a relatively easy matter to calculate the flow the theory predicts in this instance.

$$Q = \frac{gA_c}{16khL_c} \cdot \Delta P \cdot \frac{e^3}{(1-e)^2} \cdot d^2 \qquad (5)$$

Assuming a value of $k = 5.0$ (Carmen[7]) the flow predicted by Equation 5 is 193 cc/sec, compared with an empirical value of 158 cc/sec. If it is assumed that $k = 6.0$ (see Anderson & Warburton[14]) then the predicted flow is 160 cc/sec, very close to the empirical value.

[‡] Mean Fibre Diameter in this instance is defined by Projection Microscope

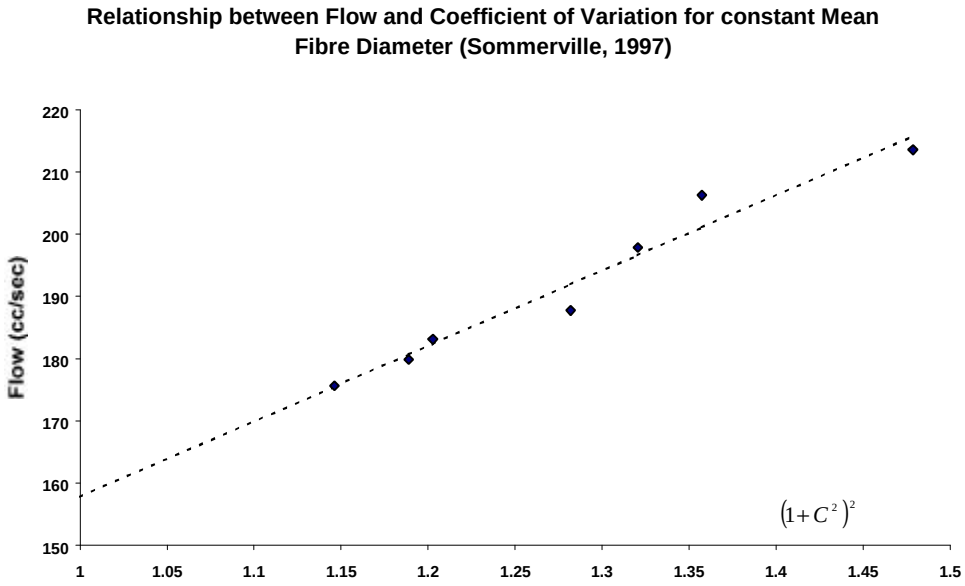

Figure 7: The data reported by Sommerville[1] has been used here to demonstrate the relationship between flow and coefficient of variation of diameter. The measured Airflow values have been converted to equivalent flows. These flows for a series of fibre blends, prepared such that the fibre diameter (as defined by the projection microscope) was a constant value (25.0 microns), is plotted as a function of the expression $(1+C^2)^2$. The dotted line is the linear regression based on these data and this has been extrapolated to the limiting value of 1.

INFLUENCE OF MEAN FIBRE DIAMETER

Equation 21 cannot be validated using the data obtained in this experiment. One of the inherent characteristics of wool is that as the mean diameter increases, so too does the standard deviation in diameter, and as a consequence, the coefficient of variation also increases, albeit by a lower percentage. Validation of Equation 21 requires a series of samples with identical coefficients of variation in diameter, but different mean diameters. If it is assumed, on the basis of Figure 8, that there is a linear relationship between flow and $(1+C^2)^2$, as predicted by the theory, then an indication of the validity of Equation can be obtained from a plot based on Equation 23.

$$Q = K_{Cd} \cdot (1+C^2)^2 \cdot \bar{d}^2 \qquad (23)$$

Equation 23 actually expresses the relationship between flow and specific surface (see Equation 3). The appropriate graphs are shown in Figure 8 (see following page).

Figure 8 indicates that the curvilinearity that has already been observed in the flow versus pressure and flow versus porosity relationships also applies to this relationship. While linear regressions can be fitted to the linear portions of the curves (see Table 2), the regression lines do not pass through zero as expected, and, as previously observed for the other relationships, these lines appear to also converge to a narrow area on the x-axis. In this case, the curvilinearity appears to be dependent on the pressure difference, and also on the magnitude of $(1+C^2)^2 \cdot \bar{d}^2$. As the magnitude of this expression decreases, the curvilinearity appears to increase. Intuitively this is to be expected. From Equation 23, as $\bar{d}$ tends to zero, so should Q. Examination of the points in Figure 8 indicates this can only occur if the curvilinearity increases. These data suggest Equation 23 (and by implication Equation 21) is an incomplete description of the relationship between flow and mean fibre diameter.

INFLUENCE OF PLUG DEPTH ON AIR FLOW

Darcy's law expresses the face velocity of the fluid, u, in terms of the pressure difference, ΔP, and the depth of the bed, L.

$$u = Constant \cdot \frac{\Delta P}{L} \qquad (24)$$

Equation 18 is a simplified version of Darcy's Law.

Figure 5, where flow is plotted as a function of pressure, shows that with respect to pressure, the Airflow instrument deviates from Darcy's law.

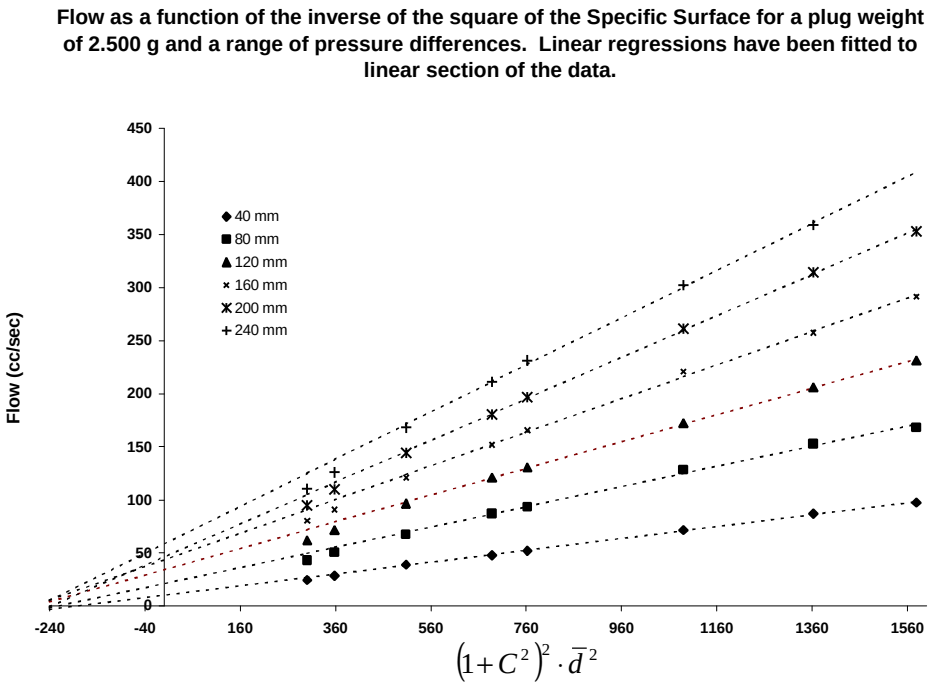

Figure 8: The flow measured by the VELOCICALC instrument has been plotted as a function of $(1+C^2)^2 \cdot \bar{d}^2$ using a constant plug mass of 2.500 g and for a range of pressure differences. If Equation 23 correctly describes the relationship then the slope of the lines should be constant, and pass through zero. However the lines are clearly curvilinear. Linear regressions have been fitted to the linear sections of these curves (corresponding to values on the x-axis greater than 360).

Table 2: Summary statistics for linear regressions fitted to Flow vs Diameter data

	Pressure Difference (mm)						
Statistic	40	80	120	160	200	240	280
R Square	0.9991	0.9962	0.9996	0.9982	0.9996	0.9987	0.995
Intercept	10.14	21.03	34.08	43.36	46.27	58.38	57.41
Std Error	0.89	3.09	1.30	3.56	1.93	4.27	10.46
Slope	0.06	0.10	0.13	0.16	0.20	0.22	0.27
Std Error	0.00	0.00	0.00	0.00	0.00	0.00	0.01

It remains to be shown whether or not the instrument adheres to Darcy's law (and hence the Kozeny equation) with respect to the depth of the plug. From Equation 24 it can be inferred that if this is the case then flow will vary directly with the inverse of the depth of the plug.

An experiment was conducted using a standard Airflow chamber and varying the plug depth by using spacers to progressively reduce the penetration of the plunger into the Airflow chamber. The porosity of the plug was maintained constant by increasing the fibre mass in proportion to the increase in the chamber volume.

This is not an easy task, due to the elasticity of the wool fibre mass. To facilitate the experiment the 25.05-micron Interwoollabs top was used, and a porosity equivalent to 2.000 grams of this top in a standard Airflow chamber was maintained. Care was taken to seal the top lip of the chamber against the circumference of the plunger, to avoid leakage of air via this route. This was achieved by placing an O-ring seal around the plunger below the lowest spacer.

The results of this experiment are shown in Figure 9 (next page), where Q is plotted as a function of $1/L$. This relationship is clearly non-linear, and demonstrates, in conjunction with Figure 5, that the Airflow instrument does not behave as predicted by Darcy's law with respect to flow and the depth of the fibre plug, although the system appears to approach linearity as the flow decreases and the depth increases.

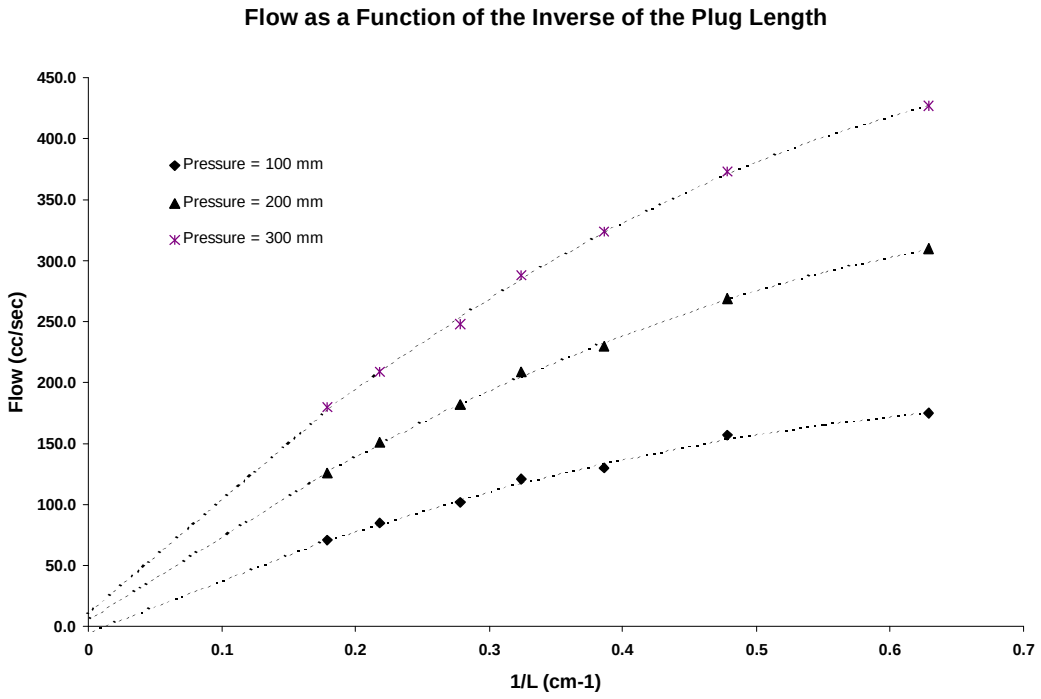

Figure 9: This figure shows the relationship between flow and the depth of the bed of wool fibre in the Airflow chamber, for a range of pressure differences. A wool top of 25.05 microns and a constant porosity equivalent to a mass of 2.000 grams of fibre in a standard Airflow chamber were used. Both Darcy's law and the Kozeny Equation predict a linear relationship between the variables. Clearly, for the range of flows and plug depths represented by these data the relationship is curvilinear. The dotted line represents a curve of best fit, based on a quadratic regression, and on the assumption that the curves pass through zero. This seems justified because the bed depth must approach infinity for the value of the x-axis to approach zero. Under such conditions a zero flow would be expected.

DISCUSSION

It is clear from the data provided by this experiment, that the Kozeny model, although describing the critical factors affecting the Airflow instrument, does not provide a complete and accurate quantitative description of the effects of these factors. In particular, the observed relationships between flow and porosity, and flow and plug depth, do not conform to predictions of the theory, with clearly curvilinear relationships being demonstrated instead of the expected linear relationships. The relationships between flow and pressure, between flow and the inverse square of the specific surface (and thereby the square of the mean fibre diameter) are more linear, but the essential curvilinear character of these relationships is still clear. The cause of these deviations from the theory must be due to some other, not yet identified, factor(s).

Three possibilities remain to be examined. Firstly the Kozeny model was developed to describe liquid flow through non-compressible beds. The Airflow instrument is based on the flow of air (a gas) through a compressible bed of fibre. Given that gases are also compressible (and expandable) it is not unreasonable to expect that the Kozeny model may need to be modified to account for these differences. Various workers have studied the specific surface of powders by measuring the flow of gases through beds of powders under standardised conditions. Alternative forms of the Kozeny Equation, allowing for the expansion of the gas as it passes through the bed, have been reported.

Secondly, the Kozeny Equation also assumes that the layer of fluid in contact with the pore boundaries is stationary, in the same way that the layer of water in contact with the surface of a closed pipe is stationary under conditions of laminar flow. However, in gaseous fluids, as the mean free path of the gas molecules becomes an appreciable fraction of the pore size, thermal agitation of the molecules can give rise to slip at the pore boundaries, which causes an increase in the flow as the pressure difference increases.

Thirdly, the physical construction and operating conditions of the Airflow instrument may be introducing factors not considered in the theory.

However, before proceeding to examine these possibilities it is necessary to establish a quantitative estimate of the Kozeny Constant, k .

QUANTIFYING THE KOZENY CONSTANT

The value of the Kozeny Constant can be calculated for each data set in Tables A1 and A2 using Equation 25.

$$k = \frac{gA_c}{16hL_c} \cdot \frac{\Delta P}{Q} \cdot \frac{e^3}{(1-e)^2} \left(1+C^2\right)^2 \cdot \bar{d}^2 \qquad (25)$$

Some results of this calculation are illustrated in Figure 10. In this instance the calculations are graphed as a function of mean diameter for a constant plug mass of 2.500g (constant porosity) and at three different pressure differences. Figure 10 demonstrates that the calculated value of k is not constant, as expected, and is also diameter dependent. Given the deviations from the theory already observed this is hardly surprising.

Lord's[28] observation that k varies with porosity and between plugs of different fibres with the same porosity has been mentioned previously.

The fact that for the Airflow instrument k is not constant partly explains the non-linearity of the various functions plotted in the preceding sections of this paper. In each case it is assumed that k is constant. However, it does appear that for specific conditions k is very nearly constant and close to the value of 5.0, as reported by Carmen[7] and that for these conditions the Kozeny Equation is a reasonable model for describing the behaviour of the Airflow instrument.

This is illustrated by Figure 11 on the following page. Here, the data in Table A2 has been inserted into the

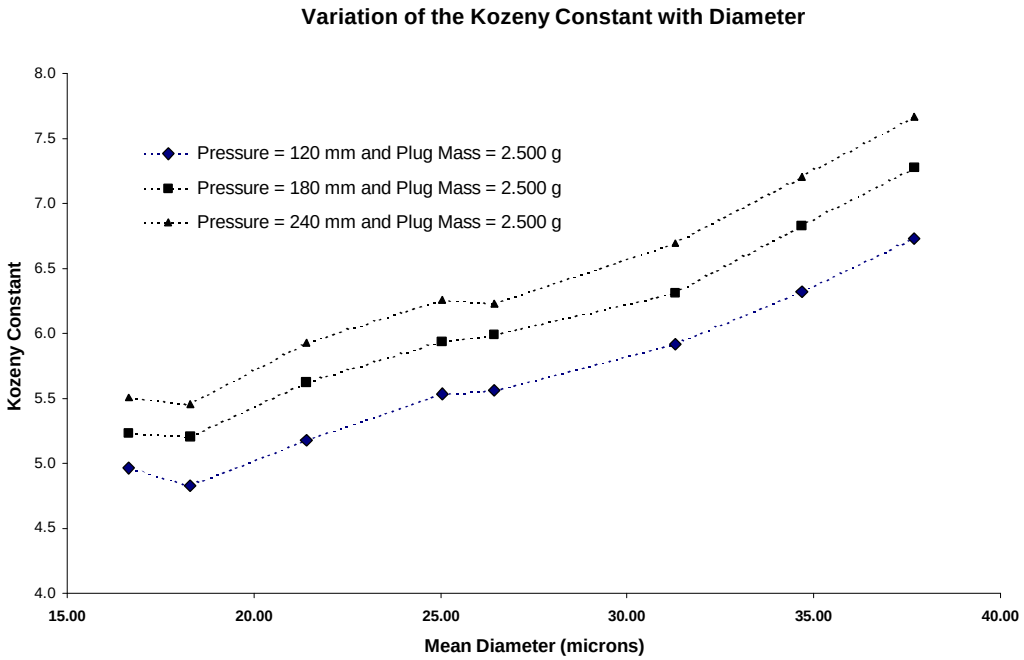

Figure 10: The Kozeny Constant has been calculated from the experimental data in Table A2 for a constant plug mass and three different pressure differences. A strong dependence with diameter is exhibited, and the value varies over a considerable range.

Anderson and Warburton[14], have also observed the diameter dependence of k. The range of k observed by these authors was somewhat smaller than shown here. However, the geometry of the chamber they used was also different from than that specified by IWTO for an Airflow instrument. Their chamber was approximately 8 mm in diameter (compared with 25.25 mm) and 35 mm deep (compared with 15.9 mm). The porosity used was very similar (approximately 0.7) and required a mass of about 0.7 grams of fibre. Anderson and Warburton did not specify the pressure differences used in making their measurements, but they used a similar system to that employed by Cassie[33], where the pressure difference was approximately 340 mm of saturated salt solution.

Kozeny Equation to calculate the flow, using $k = 5.0$, for each set of conditions represented in the table. The calculated flow has then been plotted as a function of the observed flow for each set of conditions. As the flow increases the calculated flow becomes increasingly larger than the observed flow. However, where the flow is less than approximately 100 cc/sec the 1:1 correspondence is reasonable.

A plot of $\frac{gA_c}{16hL_c} \cdot \Delta P \cdot \frac{e^3}{(1-e)^2} \left(1+C^2\right)^2 \cdot \bar{d}^2$ versus Q should give a straight line, with slope k. For flows less than 80 cc/sec this gives a value of $k = 5.5$

However, in subsequent calculations, it will be assumed that $k = 5.0$

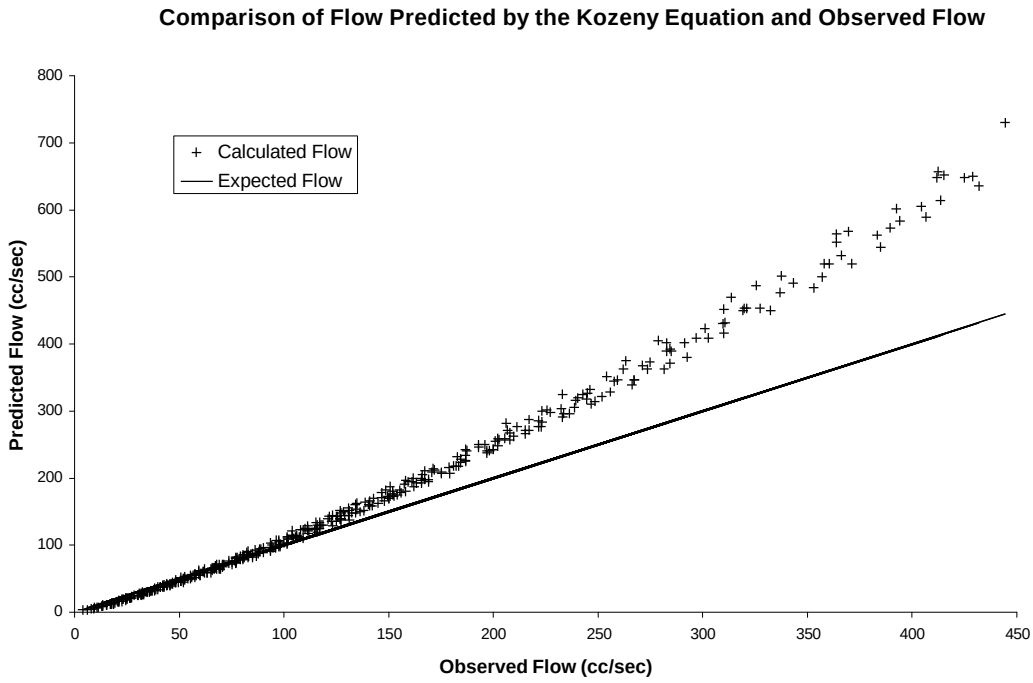

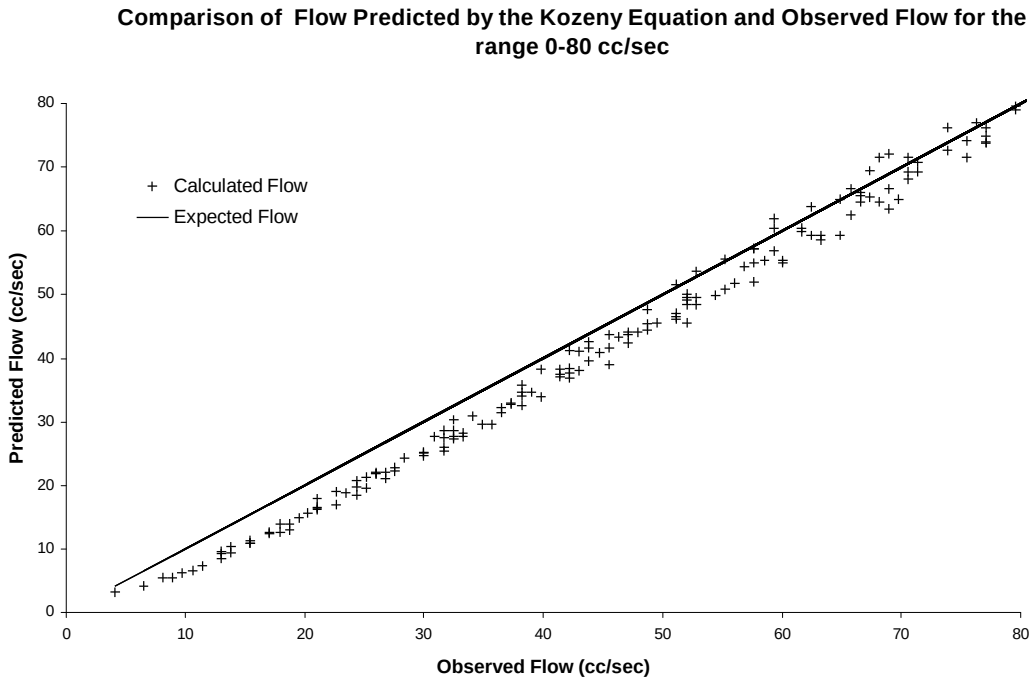

Figure 11: The data in Table A2 has been inserted in the Kozeny Equation and the flow calculated for each set of experimental conditions in the table. The calculated flow has then been plotted as a function of the actual flow measured for the particular set of conditions. The graph at the top represents all the data. The graph at the bottom represents the subset of the data for which the flow was less than 80 cc/sec. The solid line represents the 1:1 relationship between the calculated and observed flows. The value of $k = 5.0$ was used. A linear regression fitted to these data, for flows less than 80 cc/sec, gives $k = 5.5$.

CORRECTING FOR EFFECTS OF ISOTHERMAL EXPANSION OF AIR

It is conventional wisdom in Engineering Fluid Mechanics that for gas velocities less than 100 metres/sec, the gas can generally be considered to be non-compressible[35]. The air velocity through the fibre bed of the Airflow is considerably less than 100 metres/sec, so any effect of expansion, as the air passes through the bed can be expected to be very small. Referring again to the Kozeny Equation:

$$Q = \frac{gA_c}{khL_c} \cdot \Delta P \cdot \frac{e^3}{(1-e)^2} \cdot \frac{1}{S_o^2} \qquad (3)$$

In dealing with the case where a gas passes through a porous bed under the influence of a pressure difference across the bed, Equation 3 must be used in the differential form[7]:

$$u = \frac{Q}{A_c} = \frac{g}{khL_c} \cdot \Delta P \cdot \frac{e^3}{(1-e)^2} \cdot \frac{1}{S_o^2}$$

$$G = ru = \frac{g}{kh} \cdot \frac{e^3}{(1-e)^2} \cdot \frac{1}{S_o^2} \cdot r \cdot \frac{\partial P}{\partial L_c} \qquad (26)$$

For an ideal gas, $\frac{P}{r} = \frac{P_S}{r_S} =$ a constant,

Equation 26 is therefore more usefully employed in the integrated form:

$$G = \frac{g}{kh} \cdot \frac{e^3}{(1-e)^2} \cdot \frac{1}{S_o^2} \cdot \frac{\Delta(P^2)}{2L_c} \cdot \frac{r_S}{P_S} \qquad (27)$$

An alternative form of Equation 26 is sometimes used:

$$G = \frac{g}{kh} \cdot \frac{e^3}{(1-e)^2} \cdot \frac{1}{S_o^2} \cdot \frac{r_m \cdot \Delta P}{L_c} \qquad (28)$$

By assuming the gas behaves like an ideal gas,

$$\frac{r_S}{2P_S} = \frac{r_m}{(P_S + P_1)}, \qquad (29)$$

$$\Delta(P^2) = (P_S + P_1) \cdot (P_S - P_1) = (P_S + P_1) \cdot \Delta P . \qquad (30)$$

By assuming that the viscosity of the gas does not change, and expansion occurs isothermally, and also by ensuring that the flow is measured on the input side of the fibre bed, Equation 26 can be modified so that:

$$Q_i = \frac{gA_c}{khL_c} \cdot \frac{r_m}{r_S} \cdot \Delta P \cdot \frac{e^3}{(1-e)^2} \cdot \frac{1}{S_o^2} \qquad (31)$$

where Q_i = the input flow.

The ratio r_m / r_S is itself a variable, because as ΔP increases, this ratio will decrease. By implication the constant K_P in Equation 18 is, in reality, not constant, and will decrease as ΔP increases. This will contribute to the curvilinearity that has been observed in Figure 5.

The magnitude of this effect can be estimated by transforming Equation 29.

$$\frac{r_m}{r_S} = \frac{1}{2} \cdot \left(1 + \frac{P_1}{P_S}\right) \qquad (32)$$

Values for Equation 32 are shown in Table 3 for a range of pressure differences. Clearly they are very close to unity, and unlikely to completely adjust for the curvature exhibited in Figure 5. That this is indeed the case is illustrated by Figure 12, which reproduces the curve for the 1.250 gm plug mass in Figure 5, and the same curve with the correction applied to the flow. The slope of the line has increased, but the difference is barely perceptible and a considerable degree of curvilinearity of the data points, as they approach zero, remains.

From this it may be concluded that isothermal expansion of the air as it flows through the fibre mass does not account for the observed deviations of the flow from the theoretical predictions.

Table 3: Correction factors to adjust for density decreases arising from isothermal expansion

Pressure Difference (mm)	0	60	120	180	240	300
Density Ratio	1.0000	0.9971	0.9942	0.9913	0.9884	0.9855

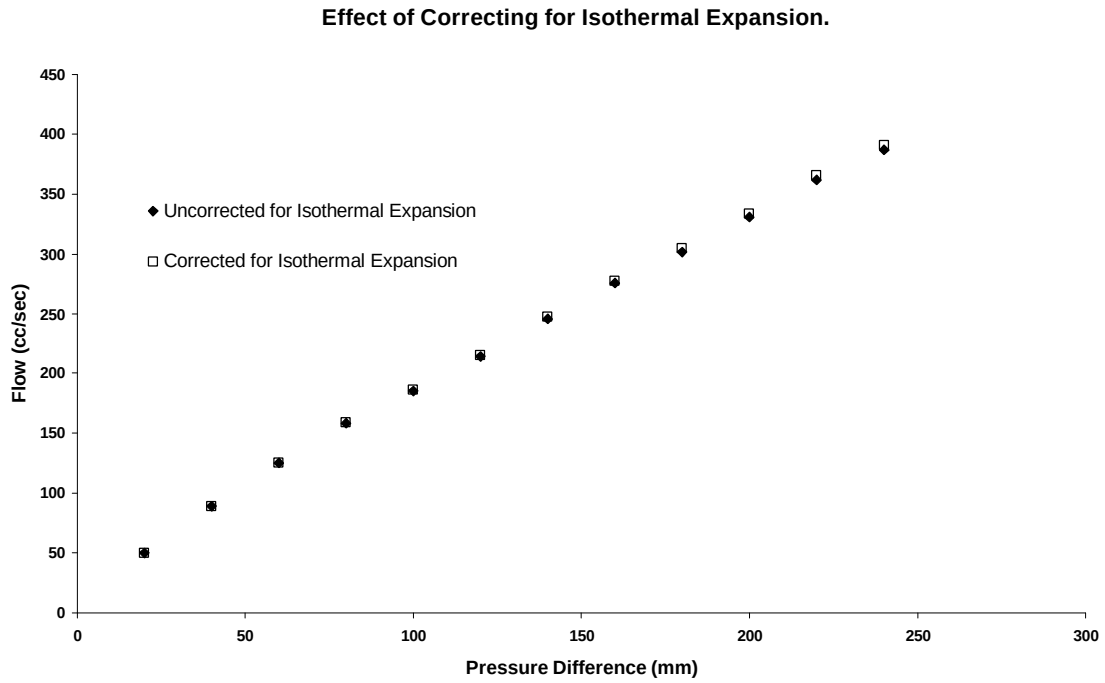

Figure 12: The flow has been corrected for the effects of isothermal expansion as the air passes through the fibre plug. The correction has been applied to the 16.66 micron sample, with a plug mass of 1.250 g, shown in Figure 5. Although there has been a small effect at the higher flows and pressures, the effect is too small to account for the observed deviations from the theoretical predictions of the Kozeny Equation.

CORRECTING FOR SLIP

Although most of the interest in the phenomenon of slip has been centred on the behaviour of gaseous fluids, the phenomenon has also been reported for liquid fluids[7]. Under situations where the flow is low, and the specific surface large, the rate of flow is observed to increase more rapidly than the drop in pressure. Two models have been postulated to explain this. The first assumes a stationary film of liquid exists at the pore surface, and this film extends out into the bulk of the pore space due to very weak intermolecular forces (such as Van der Waals forces). As the flow rate increases, the resulting frictional forces very quickly increase and rapidly break down the stationary layer. The second model assumes that a small, stationary ring of fluid is retained at each point of contact within the bed material, and the velocity of flow controls the size of this ring.

The first of these models is generally used to explain slip in gaseous systems. Carman and Arnell[36] analysed a number of models developed to quantify the effect of slip, and proposed a modification of the Kozeny Equation, which assumes the following form:

$$Q = Q_K + \frac{gA_c}{khL_c}\Delta P\left[\frac{8}{3}\sqrt{\frac{2RT}{M}}\frac{dk_0 he}{S_o(1-e)P_A}\right] \qquad (33)$$

By inserting the appropriate constants, and assuming the molecular weight of air is close to that of nitrogen (the predominant gas present), Equation 33 can be expressed as follows:

$$Q = \mathrm{K}_1\frac{1}{k}\Delta P\frac{e^3}{(1-e)^2}\frac{1}{S_o^2} + \mathrm{K}_2\frac{1}{k}\Delta P\left[\frac{e}{S_o P_A(1-e)}\right] \quad (34)$$

where $\mathrm{K}_1 = \frac{gA_c}{hL_c} =$ 1.690 x 10^7 and

$$\mathrm{K}_2 = \frac{8}{3}\cdot\frac{gA_c\, dk_0}{L_c}\cdot\sqrt{\frac{2RT}{M}} = 2.445 \text{ x } 10^5$$

For the Airflow instrument this model predicts that the phenomenon of slip will act to increase, rather than decrease the flow. This effect will be more pronounced at lower arithmetic mean pressures (or larger pressure differences), at higher porosity (lower plug weights), and at lower specific surfaces (higher mean fibre diameters). The magnitude of the correction is quite small, generally less than 2%.

Consequently, slip is not a significant factor in the deviation from the Kozeny Equation observed in this experiment.

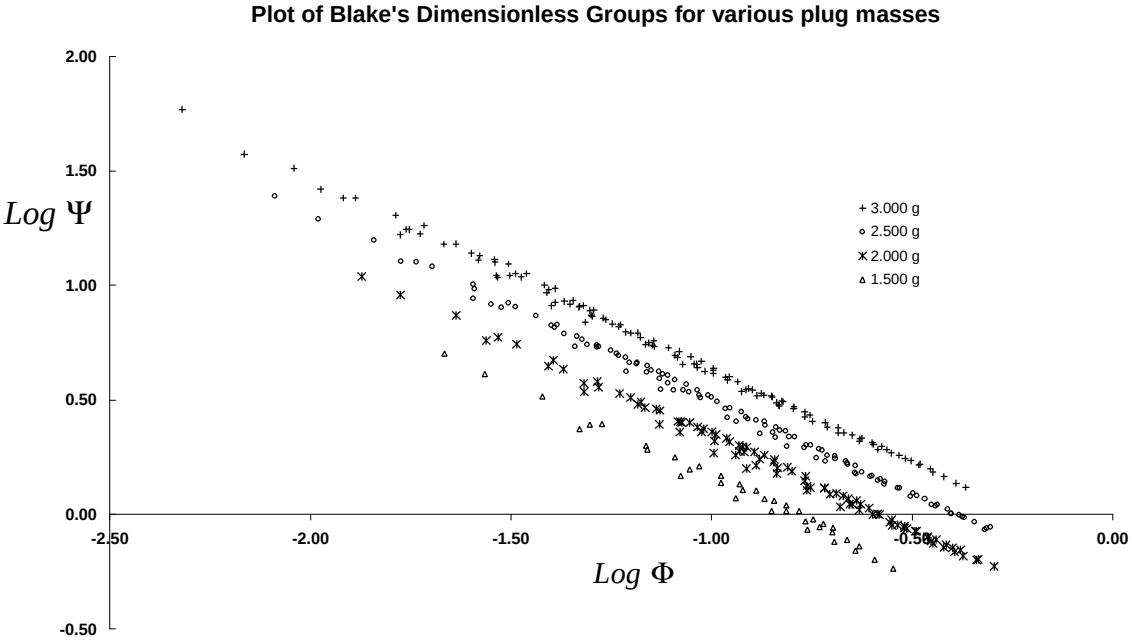

INFLUENCE OF THE DESIGN OF THE AIRFLOW

It is conceivable that that the Airflow design is the important factor in the behaviour observed in this experiment. There are several aspects of the design that can be evaluated to determine whether or not this is the case.

Laminar Flow

Kozeny's Equation is derived in part from Darcy's law and is therefore subject to the same limitations. The most important limitation is that when the ratio ru/hS_o approaches and exceeds approximately 2.0, the pressure loss across the bed rises more quickly than the flow. This is analogous to the onset of turbulent flow in a straight pipe except that in the case of porous beds the transition from laminar to turbulent flow takes place quite gradually. In such circumstances, the observed flow will be less than the predicted flow. This is precisely what is happening in the case of the Airflow when the flow exceeds 100 cc/sec. This raises the question of whether or not the instrument design is causing turbulent rather than laminar flow.

Superficially it would seem that this limitation would not apply in this instance. Using the known chamber dimensions, and the flow data from this experiment combined with the fibre diameter information, the ratio ru/hS_o can be readily calculated. None of the values so obtained exceed 2.0.

Plotting Blake's dimensionless groups[5] can readily check adherence to Darcy's law and the assumption of laminar flow. These are defined by Equations 35 and 36, and have been shown to give rise to the Kozeny Equation in the region of laminar flow[7].

$$\Phi = \frac{r \cdot u}{h \cdot S_o} \tag{35}$$

$$\Psi = \frac{\Delta P \cdot g \cdot e^3}{L_c \cdot r \cdot u^2 \cdot S_1} \tag{36}$$

Here, $S_1 = \left(S_o + \frac{4}{D} \right)$, the total surface of fibre area per unit volume, inclusive of the chamber surface and D is the diameter of the chamber

The normal practice is to plot the logarithms of Equations 35 and 36, with Equation 35 as the dependent variable. Such a plot, based on the data from Table A2 is shown in Figure 13. The data for 4 different plug masses (and hence different porosity values) has been plotted. If Darcy's law applies, and the system is in the zone of laminar flow, the plot should be linear. Non-laminar flow, where the pressure loss rises more rapidly than the flow, results in the lines curving upwards, towards the right of the graph. All these data are significantly less than the critical value of $ru/hS_o = 2.0$ (Log 2 = 0.30), and, as expected, the plots are linear. Consequently it seems reasonable to assume that the Airflow design is within the region of laminar flow.

However, the four sets of data in Figure 13 do not overlap as expected, but instead form parallel lines that are approximately equidistant on the vertical scale. This must reflect the failure of the Kozeny Equation and Darcy's Equation to adequately describe the effects of porosity on the Airflow instrument. It also suggests that some factor associated with porosity may be causing observed deviations.

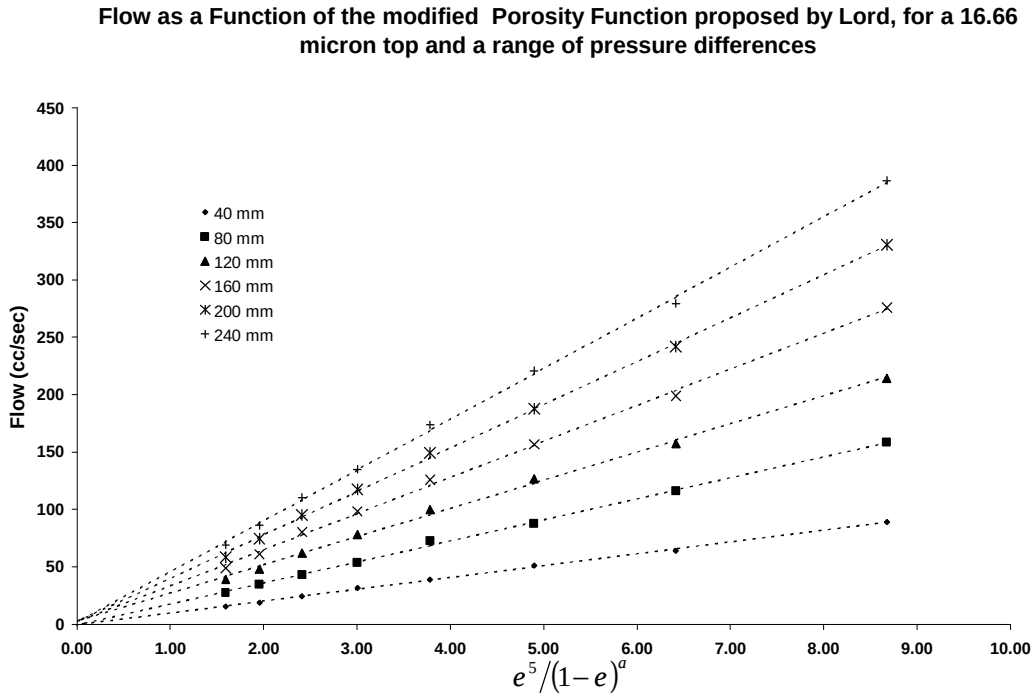

Figure 14: Lord proposed a modification to the porosity function $e^3/(1-e)^2$ of the form $e^5/(1-e)^a$ where the value of a is fibre specific, and for wool equals 1.253. A function of the form $e^3/(1-e)^a$, does effectively remove the curvilinearity (compare the above with Figure 6) but it also significantly reduces the magnitude of the porosity term in the Kozeny Equation. This requires a significant decrease in the value of k to compensate.

Porosity

Applications of the Kozeny Equation usually involve beds with a much lower porosity than occurs in the case of the Airflow instrument. Typically, the porosity of powder beds is the range 0.25 to 0.45. The Airflow is designed to operate at a porosity of 0.759.

Lord[28] proposed a modification of the porosity term in the Equation to correct for the variation he observed in the Kozeny constant as the porosity changed (see Equation 22). This adjustment can also be made to the data from this experiment. However, it results in substantially the same relationship illustrated in Figure 6, except the convergence of the regression lines is no longer on the x-axis. Figure 14 reproduces Figure 6, except the porosity term proposed by Lord has been modified to $e^3/(1-e)^a$.

On the surface this empirical adjustment is attractive, as it does appear to produce the expected linear relationships. However, it does little to resolve the real and substantial differences between the observed flows and the predicted flows, which is not unexpected because it has no theoretical foundation. This adjustment does have general application across the range of flow and porosity reported here, but its effect is really a mathematical contrivance. In reality it simply reduces the numerical magnitude of the ratio, and increases the relative magnitudes between the particular values used, increasingly so as the ratio decreases, thereby making the curves more linear. This can be seen by inspection of the x-axis in Figure 6 and in Figure 14.

Dupuit (circa 1863) introduced the concept of porosity into the theory of fluid flow through porous beds by extending Darcy's law. He realised that the actual velocity of a fluid within the pores of a porous bed must be larger than the apparent velocity through the bed. If the pore space in the bed is uniformly distributed, then the porosity of a layer of infinitesimal thickness normal to the flow must be equal to the porosity of the bed as a whole. For such a layer the fractional free volume is equal to the fractional free area, and therefore the true velocity of flow is u/e. Engineers have long used the concept of mean hydraulic radius in describing fluid flow through circular pipes.

$$R_H = \frac{Cross\ sectional\ area\ normal\ to\ flow}{Perimeter\ presented\ to\ fluid}$$

Since the cross section of a pipe is uniform an alternative expression for the mean hydraulic radius is:

$$R_H = \frac{Volume\ of\ \ fluid\ in\ pipe}{Surface\ presented\ to\ fluid}$$

If this assumption is applied to granular beds, then $R_H = e/S$. Kozeny used this assumption in deriving his equation. He assumed that a granular bed could be considered to be equivalent to a group of parallel, similar channels, in which the total internal surface and the total internal volume are equal to the particle surface and the pore volume respectively. The mean hydraulic radius for these channels is therefore e/S.

The Kozeny model was developed for non-compressible granular beds. The value of S for such beds will in fact be less than the actual surface area of the particles, because points of particle contact will not be exposed to the fluid. However, for reasonably symmetrical particles, the difference will be negligible.

A bed of wool fibre is compressible. Moreover, wool fibres are more appropriately described as flexible cylinders, rather than particles. By compressing the fibre bed the porosity is reduced, and the fibre to fibre contacts will be increased[37]. Inevitably the area of surface exposed to the gas will be less in a compressed bed than the area exposed in a more porous bed. As a consequence there will be a non-linear variation in mean hydraulic radius, and therefore a non-linear change in flow for a constant pressure difference.

The fact that the relationship between Q and $e^3/(1-e)^2$ actually approaches linearity as porosity increases (see Figure 6), supports this hypothesis. In a more porous bed of randomly oriented fibres, the change in the number of fibre to fibre contacts will be less for a uniform change in porosity than in a highly compressed bed.

The alignment of fibres in tops is known to increase the number of fibre to fibre contacts[38,39]. It has been shown experimentally that wool tops measure slightly coarser with Airflow when the fibres are disoriented.

However, this effect cannot explain the difference in calculated and observed flow exhibited in Figure 11. For high flows, which are generally associated with higher differences in pressure, lower specific surfaces (higher mean diameter) and/or lower porosity, the calculated flow is almost twice the observed flow. This would require a 40% decrease in the Specific Surface, which could only arise from a large increase in the number of fibre to fibre contacts. This could not occur if the porosity is increasing - the opposite would occur. Also, the non-linearity of the flow relationships occurs in situations where the porosity of the fibre bed is maintained constant, and hence the number of fibre to fibre contacts is also constant.

Nevertheless, the increase in fibre to fibre contacts resulting from compression is probably contributing to the non-linearity observed at low pressures and where the porosity is increasing, as illustrated by Figure 6. However, this effect is likely to be relatively small, and certainly not sufficient to explain the experimental data.

Pressure Losses

The Kozeny Equation has been demonstrated to be a reasonable model for describing the flow of fluids through granular beds, and also beds of fibres such as cotton. However, it does not describe the Airflow instrument with the same completeness. The clues as to why this is so are contained in Figures 6 and 9 and particularly in the latter.

The Airflow instrument differs in one very critical area from measurements of flow characteristics through granular beds. Plugs of wool fibre are compressible. Powders are not compressible. Accordingly, the instrument requires a plunger to compress the fibre to a standard volume. This plunger has a perforated base, where each hole has a nominal diameter of 1.5 mm.

The importance of the dimensional characteristics of the instrument and in particular the importance of the size and distribution of these holes has been previously recognised[40,41].

Effectively, the air has to move through a much smaller area than the cross-sectional area of the bed before it can even begin to flow through the bed. The total area of these holes in the instrument used for this experiment was approximately 21% of the area of the chamber. Hence, if it is assumed that the flow is isothermal and compression does not occur, the average face velocity through each hole in the plunger will be approximately 5 times the face velocity through the bed itself. Similarly, as the air exits the bed through the base of the chamber the average face velocity must again increase by a factor of approximately 5.

The effect of porosity on the flow of air through the perforations in the base of the plunger and in the base of the chamber is clearly quite important. It was observed during this experiment that the flow of air through these perforations was substantially unimpeded when the chamber was empty. There is not a significant difference in flow when the plunger is inserted and when it is removed. When wool fibre is present, the average porosity within the chamber will be constant, but the air entering the chamber must initially flow through the tortuous channels within the plug at a velocity at least 5 times greater than the would be otherwise necessary. This velocity will reduce as the air penetrates deeper into the fibre mass.

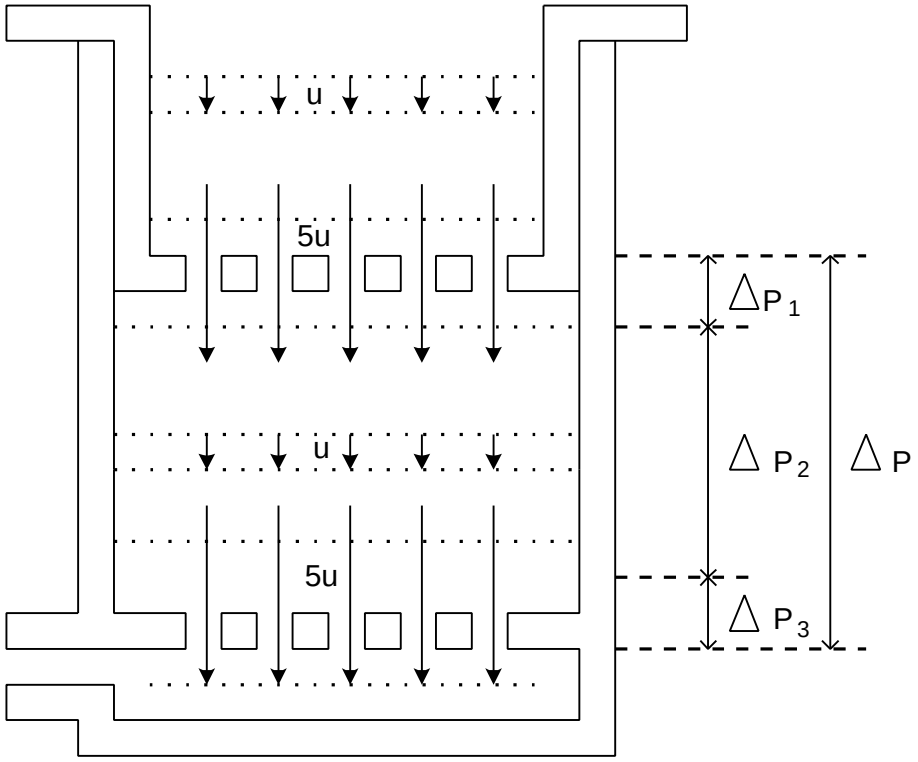

Figure 15: This is a schematic representation of the fluid hydraulics of the Airflow instrument. It is not to scale. Effectively the instrument can be segmented into 4 separate zones. The first zone is above the plunger where the vector u represents the face velocity. The second is where the air passes through the base of the plunger and the vector $5u$ represents the maximum face velocity. The third zone is within the chamber itself where the face velocity returns to u. Finally as the flow exits the base the face velocity rises again to $5u$. The resultant pressure changes are also indicated by ΔP_1, ΔP_2, ΔP_3, and ΔP.

As indicated in Figure 15, this effect gives rise to a resistance to flow over and above the resistance arising from the bed itself. The magnitude of this resistance will vary, in direct proportion to the flow. The effect will be to reduce the flow below that predicted. This effect is likely to be complex, being dependent upon the porosity, the specific surface and the overall pressure difference.

Consider Figure 15. In the Airflow instrument, the pressure difference across the compressed bed of fibre must be considered to consist of three components:

$$\Delta P = \Delta P_1 + \Delta P_2 + \Delta P_3 \qquad (35)$$

where ΔP_1 = pressure drop across the base of the plunger;

ΔP_2 = pressure drop across the fibre bed; and

ΔP_3 = pressure drop across the base of the chamber.

The pressure difference ΔP is externally applied. If ΔP_1 and ΔP_3 increase, then ΔP_2 must decrease. Assuming that flow in this zone is described by the Kozeny Equation, then it follows that the rate of flow through the zone will be lower than in the entry and exit zones.

For conditions where the flow is very low, ΔP_1 and ΔP_3 are likely to be small compared to ΔP_2, so that $\Delta P_2 \approx \Delta P$. This accounts for the closer compliance with the theory at low flows. It should be noted that studies of flow through fibre beds, which have reported substantial compliance of experimental systems with Blake's law and with the Kozeny Equation (Lord[28], Fowler and Hertel[10]), have, in the main, confined the measurements to very low-pressure differences and very low flows.

Conversely, for a constant porosity, as flow is increased, by increasing the pressure differential ΔP, ΔP_1 and ΔP_3 will increase, causing reduction of the observed flow compared with the predicted flow. The magnitudes of ΔP_1 and ΔP_3 are a function of pressure, porosity and specific surface.

This model also explains the deviations from Darcy's law illustrated by Figure 9. In this case the porosity is constant but the bed depth is increasing. The curvilinearity of the lines represented in this example increases significantly for higher differences in pressure. Higher pressures result in higher flows and therefore increases in ΔP_1 and ΔP_3. The near linearity

of the Airflow calibration can be explained by the assumption that in the limiting case, as the flow increases, ΔP_1 and ΔP_3 becomes relatively constant, and the flow then begins to adhere to Darcy's Law.

The complexity in describing this model in mathematical terms arises from the fact that the depth of the three zones over which these pressure changes occur will vary with porosity, specific surface and pressure. Such a description is being developed, and hopefully will provide some basis for the design of experiments that can validate the model.

COMMERCIAL IMPLICATIONS

The Airflow instrument is a calibrated instrument. As a consequence, whether or not it behaves as predicted by the theory is of no great significance. However, this only remains the case while measurements using the instrument are limited to the calibrated range of the instrument.

This experiment has shown that the behaviour of the Airflow instrument deviates from theory, particularly with respect to pressure, porosity and fibre diameter. It has been postulated that these deviations are due to the mechanical design of the instrument rather than any deficiency in the theory per se.

The Airflow instrument operates over a quite wide range of flow (50 – 350 cm^3/sec) at a pressure difference in the middle of the range investigated here. As a consequence, the calibration curve for the instrument is determined by a complex array of factors, including the flow characteristics of the rotameter. This has resulted in a calibration curve that is very nearly but not quite linear over the range of the calibration tops.

In the flow range 0-100 cc/sec the instrument is reasonably described by the theory - flow is proportional to diameter squared. For superfine wool, less than 19 microns, the airflow through the instrument is within this range of closest conformance with the theory. However, the shape of the calibration curve is largely determined by flow determining factors that are in the range where the instrument does not conform to the theory. Thus the calibration is largely fitted to a region where the flow/diameter relationship is nearly linear. However, as the fibre becomes increasingly finer than 19 microns, the flow/diameter relationship becomes increasingly non-linear.

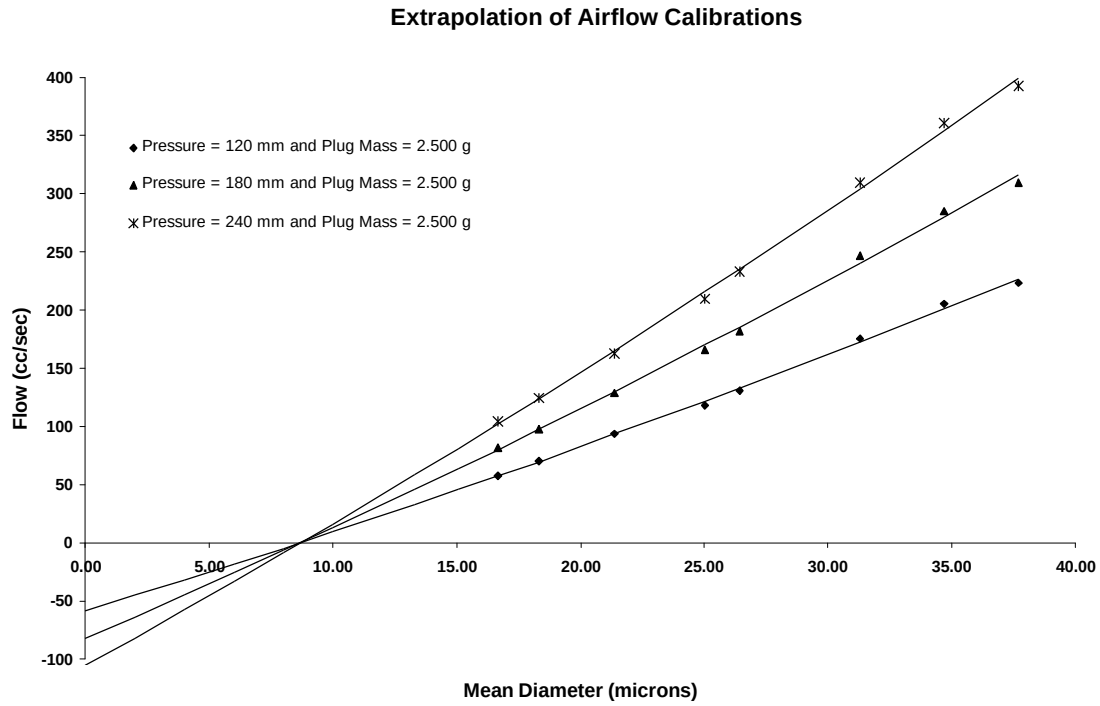

Figure 16: The Airflow calibration points for the IH Tops have been plotted for three different pressures and a standard plug mass of 2.500g. The regressions to these points have been determined using the procedures in IWTO-28 and the resultant curves extrapolated to cut the x-axis. The curves all intersect on the axis at a point equivalent to 8.70 microns.

Table 4: Effect of using LASERSCAN and OFDA data to extend the range of diameters used to calibrate the Airflow

		Measured Diameters	Diameters Calculated from Regressions		
			120 mm	180 mm	240 mm
Intercept with x-axis	IH Tops		8.70	8.70	8.71
	IH Tops + LASERSCAN		7.71	7.70	7.52
	IH Tops+ OFDA		6.21	6.20	5.98
Diameters for Fleeces	IH Tops	13.85	13.95	13.92	13.96
	IH Tops + LASERSCAN	13.32	13.50	13.45	13.41
	IH Tops+ OFDA	12.49	12.90	12.85	12.79
	IH Tops	15.46	15.51	15.58	15.77
	IH Tops + LASERSCAN	15.06	15.17	15.24	15.37
	IH Tops+ OFDA	14.55	14.75	14.82	14.97

Figure 16 shows three calibration curves for the Airflow instrument used in this study. These data have been taken from Table A2. The actual recorded flows have been used instead of the rotameter heights. The data corresponding to the normal operating mode of the instrument ($\Delta P = 180$-mm) have been used, as well as data corresponding to pressure differences of 120-mm and 240-mm. The curves are very nearly linear and have been extrapolated to cut the x-axis. They do not pass through zero, as one would expect they should, but instead converge to a point on the x-axis equivalent to 8.70 microns. This suggests that as the mean diameter reduces below 16.66 microns (the finest calibration top) the instrument will read increasingly coarser than the "true" diameter.

It is known that for Australian superfine wool both LASERSCAN and ODFA are finer than the Airflow[42]. The extrapolation errors associated with the Airflow instrument for these wools may account for these differences.

Tables A3 and A4 in Appendix A show the same flow data for two very fine fleeces obtained from a superfine wool flock in New South Wales. Both samples were measured using LASERSCAN and OFDA. These data were incorporated with the data used for Figure 16, and the regression lines for each extended set of flow readings calculated incorporating the respective mean diameters of these fleeces obtained by both instruments. Table 4 summarises some of the information that can be extracted from these calculations. The "calibration curves" so obtained are very similar to those shown in Figure 16, and are shown in Figure 17 (see next page).

As expected, because LASERSCAN and OFDA both measured the fleece samples as being finer than the corresponding Airflow measurements, the intersection of the LASERSCAN and the OFDA "calibration" sets with the x-axis is closer to, but not equal to zero. When the diameters of the fleece samples are obtained from the respective calibration curves they are close to the actual values obtained when they were originally measured with LASERSCAN and OFDA. There is nothing surprising in this. It simply illustrates the effect of extending the Airflow calibrations with wool samples that have a mean diameter less than they would measure using the extrapolated IH top calibration. However Figure 17 does illustrate that even if the fine fleece samples are included, fitting the flow and diameter data to a quadratic equation still results in a non-zero intercept with the x-axis.

The calibration curves for the data corresponding to a 180-mm pressure difference are shown in Figure 17. These data should not be interpreted as validating the LASERSCAN and/or the OFDA measurements. Calibrations for both of these instruments must also be extrapolated to measure diameters less than 16 microns. However they could be interpreted as an indication that the Airflow instrument probably provides results which are slightly coarser than the "true" result as the mean diameter decreases below 16 microns. The likely magnitude of this effect is sufficient to explain a significant proportion of the differences from the other instruments that have been reported for these wools. The commercial impact of this effect is likely to be small, since the quantity of wool produced in this range of diameters is very small.

This effect is also likely to cause difficulties in using variable plug masses in the Airflow instrument when measuring wool finer than 16.66 microns. In this region the calibrations need to be extrapolated and it is unlikely that such extrapolations will be sufficiently accurate or sufficiently robust. Conversely, because of the linearity exhibited by the system as the diameter increases, it is probable that variable plug mass calibrations will be robust when extrapolating above 38 microns.

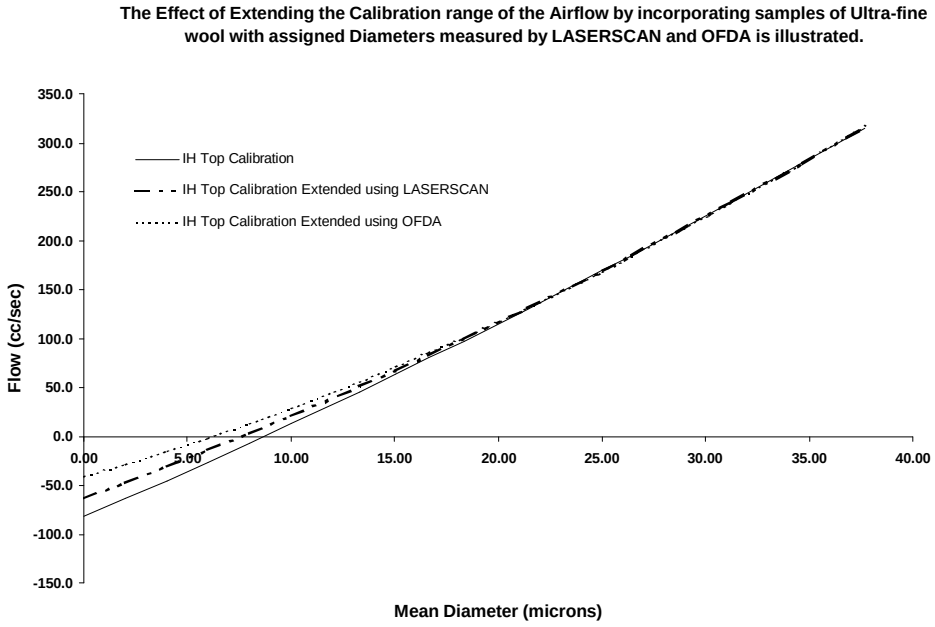

Figure 17: The three calibration curves used to obtain the data presented in Table 4 are shown here. The strength of the influence of the assigned values of the IH tops on the curves is quite apparent in the extrapolated region, despite the addition of the LASERSCAN and OFDA data.

CONCLUSION

This experiment has demonstrated that the Kozeny Equation does not completely describe the behaviour of the Airflow instrument, despite the theory frequently being quoted in the literature in relation to various aspects of fibre fineness measurement by the instrument. Divergence between theory and practice, over the ranges in flow and pressure normally utilised in the Airflow instrument, has been observed for all the significant variables, including:

- Effect of pressure differences;
- Effect of porosity differences; and
- Effect of specific surface (or mean fibre diameter).

The one variable where the theory seems to predict the effect with reasonable accuracy is Coefficient of Variation. This may only be due to the restricted range of data available to test the predictions of the theory.

Theory and observation are most closely aligned at flows below 100 cm^3/sec. However, even in this range the trends that extend across the observed range of flow, porosity, pressure difference and mean diameter are also present in the data.

The possibility that isothermal expansion or the phenomenon of slippage may be contributing factors to the observed deviations has been investigated. Although these factors do contribute they are not the major cause. Likewise, the incidence of fibre to fibre contacts in the compressed bed of fibre probably contributes to the deviations in the circumstances when porosity is low and the flows are also low, but this is also believed to be a relatively minor effect.

It is likely that the differences between theory and practice are due to the same cause in all cases. It has been postulated that the mechanical construction of the Airflow chamber, where a perforated base plate and a perforated plunger are used to compress the fibre mass to a constant volume, may be the major contributing cause of these differences. This construction forces rapid changes in face velocity of the air as it enters and leaves the chamber. This causes resistance to flow, for particular pressure differences, above that which is due to the mass of fibre in the chamber. Further investigation of this hypothesis is proposed.

If this is the case, then it has some implications regarding the use of the Airflow instrument for measuring fibre diameter outside the range of the calibration tops, and in particular for very fine wools. The instrument is likely to be biased slightly coarser in this area of extrapolation. It also has implications for the use of variable plug weights for the measurement of ultra-fine wool. It is unlikely that the extrapolations required to do this will be sufficiently robust and certainly they will be less robust than using constant masses. However, for coarse wools the variable plug mass procedure is likely to be quite robust, due to the linearity of the flow versus porosity and flow versus diameter relationships for coarser wools.

ACKNOWLEDGEMENTS

The author particularly wishes to recognise the contribution of P. C. Carman[7] to the content of this document. Much of the material included here has been drawn from his work. The assistance of Laurie Parr in providing the engineering support required build the apparatus used is gratefully acknowledged, as is the contribution of Florentina Fernandez, Chris Abela, Lorraine O'Rourke and Craig Davey, each of whom assisted in preparing and conditioning the samples used in this study. The author also acknowledges the contribution of Peter Baxter in reviewing the original draft of the paper, and the contributions of Jim Marler and Trevor Mahar to the many long and useful discussions about the interpretation of the results obtained.

APPENDIX A

Table 1: Summary of Airflow Measurements derived from VELOCICALC readings

			ELECTRONIC FLOW METER READINGS (cc/sec)															
MFD	CVD	Mass	PRESSURE DROP (mm)															
			0	20	40	60	80	100	120	140	160	180	200	220	240	260	280	300
16.66	0.1998	1.250	0.0	49.1	87.1	121.9	154.3	181.3	209.0	239.8	269.1	294.4	322.1	353.0	376.8			
		1.500	0.0	35.6	62.5	87.9	113.2	133.8	153.6	174.1	193.9	212.9	235.9	253.3	272.3	295.2	313.4	330.8
		1.750	0.0	27.7	49.9	68.1	85.5	106.1	123.5	137.7	152.8	167.8	182.8	197.9	215.3	228.0	241.4	260.4
		2.000	0.0	22.2	38.0	53.8	70.4	86.3	97.4	110.0	122.7	137.7	145.6	157.5	169.4	182.8	193.1	201.8
		2.250	0.0	17.4	30.9	41.9	52.2	64.1	76.0	85.5	95.8	104.5	114.8	124.3	131.4	140.9	150.4	160.7
		2.500	0.0	13.5	23.7	33.2	41.9	51.4	60.2	68.1	78.4	85.5	92.6	100.5	107.6	114.0	121.9	128.2
		2.750	0.0	10.3	18.2	26.1	34.0	39.6	46.7	54.6	59.4	64.9	72.8	79.2	83.9	87.9	97.4	101.3
		3.000	0.0	7.9	15.0	21.4	26.9	31.7	38.0	43.5	47.5	51.4	57.0	63.3	67.3	74.4	79.2	83.9
18.31	0.1821	1.500	0.0	41.2	75.2	104.5	133.0	159.1	180.5	204.2	231.9	258.8	281.0	302.4	328.5	353.0		
		1.750	0.0	32.5	57.0	79.9	102.1	121.1	144.1	160.7	176.5	193.1	211.3	232.7	250.9	265.9	285.7	305.5
		2.000	0.0	25.3	44.3	60.9	78.4	95.0	110.0	127.4	139.3	151.2	164.6	180.5	193.1	204.2	216.9	233.5
		2.250	0.0	19.8	34.8	48.3	61.7	76.0	87.1	98.1	108.4	122.7	133.8	143.3	152.0	162.3	174.9	183.6
		2.500	0.0	15.8	27.7	38.8	49.1	60.2	69.7	79.2	88.6	98.1	106.9	114.0	122.7	130.6	139.3	148.0
		2.750	0.0	12.7	23.0	31.7	39.6	47.5	56.2	63.3	63.3	78.4	85.5	91.0	96.6	105.3	114.0	118.7
		3.000	0.0	10.3	18.2	26.1	32.5	38.0	43.5	50.7	58.6	64.9	70.4	75.2	82.3	88.6	95.0	100.5
21.40	0.2303	1.500	0.0	59.4	106.1	145.6	178.9	220.0	256.4	289.7	323.7	359.3						
		1.750	0.0	43.5	79.2	111.6	136.9	163.0	186.8	212.1	241.4	267.5	289.7	314.2	338.8	368.0		
		2.000	0.0	34.8	60.9	83.1	104.5	129.0	148.8	167.0	181.3	201.0	217.7	242.2	259.6	277.8	291.3	312.6
		2.250	0.0	26.9	42.7	67.3	84.7	103.7	121.1	135.3	148.8	164.6	177.3	196.3	207.4	222.4	234.3	249.3
		2.500	0.0	21.4	38.0	51.4	65.7	79.2	94.2	107.6	117.9	126.6	140.9	150.4	163.8	171.8	183.6	193.9
		2.750	0.0	17.4	30.9	41.2	51.4	64.9	76.0	85.5	95.0	103.7	113.2	125.1	133.0	141.7	148.0	156.7
		3.000	0.0	13.5	23.7	33.2	41.2	49.9	59.4	68.1	75.2	83.1	91.0	98.9	105.3	112.4	119.5	128.2
25.05	0.2171	1.750	0.0	53.8	96.6	134.6	169.4	197.9	227.2	264.4	295.2	327.7	357.0	382.3	411.6	444.0		
		2.000	0.0	42.7	74.4	102.9	131.4	159.1	186.0	208.2	231.9	256.4	284.9	306.3	330.1	353.0	376.8	395.8
		2.250	0.0	35.6	60.9	85.5	106.1	126.6	148.0	170.2	188.4	205.8	226.4	243.0	264.4	284.9	303.1	319.0
		2.500	0.0	27.7	46.7	63.3	84.7	102.1	117.9	133.0	148.0	161.5	175.7	192.3	205.8	220.8	235.1	248.5
		2.750	0.0	23.0	39.6	57.0	72.0	85.5	98.1	110.8	126.6	140.1	149.6	158.3	167.8	179.7	192.3	201.0
		3.000	0.0	18.2	31.7	44.3	54.6	66.5	78.4	89.4	100.5	110.0	117.9	126.6	137.7	147.2	153.6	163.0
26.43	0.2116	1.750	0.0	60.2	105.3	147.2	186.0	218.5	250.1	284.1	322.1	353.8	386.3	415.5				
		2.000	0.0	49.9	86.3	118.7	150.4	178.9	204.2	231.9	261.2	288.1	312.6	332.4	364.9	392.6	417.1	0.0
		2.250	0.0	38.0	66.5	94.2	115.6	140.9	163.8	186.8	204.2	224.8	243.8	262.8	288.9	308.7	328.5	344.3
		2.500	0.0	29.3	50.7	71.2	91.0	106.9	127.4	147.2	161.5	178.1	191.5	210.5	225.6	245.4	259.6	273.1
		2.750	0.0	23.7	40.4	57.8	73.6	89.4	103.7	116.4	132.2	144.8	155.1	167.0	178.1	191.5	202.6	213.7
		3.000	0.0	18.2	32.5	45.9	58.6	72.0	83.9	95.0	104.5	114.8	128.2	137.7	146.4	155.9	166.2	176.5
31.28	0.2354	2.000	0.0	64.1	111.6	152.8	191.5	224.8	265.2	299.2	332.4	361.7	399.7					
		2.250	0.0	51.4	91.8	129.0	163.0	195.5	222.4	250.1	279.4	308.7	339.6	360.9	386.3			
		2.500	0.0	39.6	69.7	99.7	125.1	147.2	167.8	189.2	215.3	234.3	254.9	274.7	294.4	315.8	335.6	357.8
		2.750	0.0	31.7	53.8	75.2	96.6	114.0	136.1	153.6	170.2	186.0	201.0	213.7	235.9	250.9	266.7	281.0
		3.000	0.0	25.3	43.5	61.7	78.4	95.0	112.4	127.4	138.5	152.0	166.2	178.9	193.9	205.0	217.7	229.5
34.69	0.2532	2.000	0.0	78.4	133.8	180.5	224.8	267.5	308.7	354.6	391.8							
		2.250	0.0	52.2	105.3	144.1	177.3	207.4	243.0	276.2	309.5	334.8	365.7					
		2.500	0.0	47.5	84.7	119.5	148.8	177.3	201.0	225.6	250.9	279.4	306.3	326.1	349.8	376.0		
		2.750	0.0	37.2	68.9	95.8	119.5	137.7	161.5	181.3	203.4	222.4	242.2	262.8	283.4	300.8	317.4	338.0
		3.000	0.0	30.9	53.0	74.4	94.2	112.4	132.2	150.4	165.4	181.3	196.3	211.3	227.2	243.0	256.4	271.5
37.69	0.2326	2.000	0.0	87.9	150.4	202.6	256.4	304.7	346.7									
		2.250	0.0	69.7	125.1	167.8	205.8	250.9	284.9	321.3	356.2							
		2.500	0.0	53.8	95.0	131.4	163.8	193.9	225.6	254.1	284.1	307.1	344.3	356.2				
		2.750	0.0	42.7	76.8	106.1	133.8	159.9	183.6	207.4	231.1	254.1	275.4	296.8	321.3	338.8	357.8	371.2
		3.000	0.0	34.8	60.9	85.5	106.1	128.2	148.8	167.8	186.8	201.8	218.5	236.7	256.4	273.1	292.9	309.5

Table A2: Summary of Airflow Measurements derived from VELOCICALC readings

			ELECTRONIC FLOW METER READINGS (cc/sec)															
MFD	CVD	Mass	PRESSURE DROP (mm)															
			0	20	40	60	80	100	120	140	160	180	200	220	240	260	280	300
16.66	0.1998	2.000	0.0	21.1	38.2	52.8	68.2	82.0	96.6	110.4	121.8	134.0	146.9	158.3	171.3	182.7	195.7	207.8
		2.500	0.0	13.0	22.7	31.7	39.8	48.7	57.6	65.8	73.9	82.0	89.3	97.4	103.9	111.2	116.9	125.0
		3.000	0.0	8.9	15.4	21.1	26.0	32.5	37.3	41.4	47.1	52.0	56.8	61.7	67.4	71.4	77.1	81.2
18.31	0.1821	2.000	0.0	25.2	43.8	62.5	80.4	97.4	111.2	127.5	142.9	157.5	172.1	186.7	201.3	211.1	227.3	240.3
		2.500	0.0	15.4	27.6	38.2	49.5	59.3	70.6	79.6	88.5	98.2	106.4	115.3	125.0	134.0	141.3	150.2
		3.000	0.0	10.6	18.7	25.2	31.7	38.2	45.5	52.0	57.6	63.3	69.8	75.5	80.4	86.9	93.4	98.2
21.40	0.2303	2.000	0.0	32.5	59.3	82.8	103.9	126.7	148.6	167.2	187.5	207.0	225.7	246.0	262.2	284.2	301.2	320.7
		2.500	0.0	21.1	36.5	52.8	66.6	80.4	93.4	105.5	116.9	129.1	140.5	151.8	163.2	175.4	186.7	198.1
		3.000	0.0	13.0	24.4	33.3	42.2	51.1	60.1	68.2	77.1	85.2	93.4	101.5	108.8	116.1	123.4	131.5
25.1	0.2171	2.000	0.0	43.0	77.9	108.8	138.8	166.4	193.2	216.8	245.2	271.2	297.1	319.1	343.4	366.2	389.7	413.2
		2.500	0.0	26.0	45.5	66.6	85.2	102.3	118.5	134.8	151.8	165.6	181.0	197.3	209.5	223.3	238.7	255.7
		3.000	0.0	17.0	30.0	41.4	54.4	65.8	77.1	87.7	98.2	107.2	116.9	127.5	136.4	145.3	154.3	162.4
26.4	0.2116	2.000	0.0	48.7	88.5	122.6	155.1	186.7	215.1	244.4	273.6	302.8	327.2	357.2	384.8	406.7	431.9	
		2.500	0.0	28.4	52.0	73.9	93.4	111.2	130.7	150.2	165.6	181.9	199.7	215.1	233.0	248.4	266.3	281.7
		3.000	0.0	18.7	32.5	45.5	58.5	71.4	83.6	95.0	104.7	116.1	126.7	138.0	147.8	158.3	168.9	179.4
31.3	0.2354	2.000	0.0	64.9	116.1	160.8	202.2	242.7	282.5	319.9	358.0	393.8	424.6					
		2.500	0.0	38.2	70.6	99.9	126.7	152.6	175.4	199.7	221.6	246.8	267.1	292.3	310.1	332.1	353.2	371.0
		3.000	0.0	24.4	43.8	63.3	79.6	97.4	112.0	127.5	142.1	155.9	168.9	183.5	197.3	207.8	222.5	236.3
34.7	0.2532	2.000	0.0	77.1	134.8	186.7	233.0	278.5	325.6	369.4	411.6	444.1						
		2.500	0.0	46.3	85.2	117.7	149.4	178.6	205.4	232.2	259.0	285.0	310.9	336.9	360.5	383.2	404.3	428.7
		3.000	0.0	30.0	52.8	75.5	95.8	114.5	132.3	151.0	167.2	184.3	202.2	216.8	233.8	251.7	267.1	284.2
37.7	0.2326	2.000	0.0	88.5	151.0	206.2	263.0	313.4	363.7	412.4								
		2.500	0.0	52.0	94.2	128.3	161.6	193.2	223.3	254.1	282.5	310.1	337.7	363.7	392.1	414.9		
		3.000	0.0	32.5	57.6	82.8	103.9	125.8	146.9	165.6	184.3	203.0	221.6	239.5	257.4	274.4	291.5	309.3

Table A3:

Summary of Airflow Measurements derived from VELOCICALC readings for two ultra-fine fleeces. The mean diameter and Coefficient of Variation in Diameter was determined by LASERSCAN

LASERSCAN			ELECTRONIC FLOW METER READINGS (cc/sec)															
MFD	CVD	Mass	PRESSURE DROP (mm)															
			0	20	40	60	80	100	120	140	160	180	200	220	240	260	280	300
13.3	**0.2072**	2.000	0.0	13.8	24.4	34.1	42.2	51.1	59.3	69.0	77.1	86.1	93.4	101.5	108.0	115.3	123.4	130.7
		2.500	0.0	8.1	15.4	21.1	26.0	31.7	37.3	42.2	47.1	52.0	57.6	61.7	66.6	70.6	76.3	80.4
		3.000	0.0	4.1	9.7	13.8	17.0	20.3	23.5	26.8	30.0	33.3	36.5	39.0	42.2	44.7	47.9	51.1
15.1	**0.2178**	2.000	0.0	17.9	30.9	43.8	55.2	67.4	79.6	90.1	101.5	111.2	121.0	131.5	141.3	151.8	159.1	170.5
		2.500	0.0	11.4	19.5	27.6	34.9	41.4	48.7	56.0	62.5	69.0	77.1	82.8	90.1	95.8	101.5	106.4
		3.000	0.0	6.5	13.0	17.9	22.7	26.8	31.7	35.7	39.8	43.0	47.1	51.1	55.2	60.1	64.9	69.0

Table A4:

Summary of Airflow Measurements derived from VELOCICALC readings for two ultra-fine fleeces. The mean diameter and Coefficient of Variation in Diameter was determined by OFDA

OFDA			ELECTRONIC FLOW METER READINGS (cc/sec)															
MFD	CVD	MASS	PRESSURE DROP (mm)															
			0	20	40	60	80	100	120	140	160	180	200	220	240	260	280	300
12.5	**0.2314**	2.000	0.0	13.8	24.4	34.1	42.2	51.1	59.3	69.0	77.1	86.1	93.4	101.5	108.0	115.3	123.4	130.7
		2.500	0.0	8.1	15.4	21.1	26.0	31.7	37.3	42.2	47.1	52.0	57.6	61.7	66.6	70.6	76.3	80.4
		3.000	0.0	4.1	9.7	13.8	17.0	20.3	23.5	26.8	30.0	33.3	36.5	39.0	42.2	44.7	47.9	51.1
14.6	**0.2220**	2.000	0.0	17.9	30.9	43.8	55.2	67.4	79.6	90.1	101.5	111.2	121.0	131.5	141.3	151.8	159.1	170.5
		2.500	0.0	11.4	19.5	27.6	34.9	41.4	48.7	56.0	62.5	69.0	77.1	82.8	90.1	95.8	101.5	106.4
		3.000	0.0	6.5	13.0	17.9	22.7	26.8	31.7	35.7	39.8	43.0	47.1	51.1	55.2	60.1	64.9	69.0

REFERENCES

[1] P. J. Sommerville, IWTO Technology & Standards Committee, Report No. 14, Boston, May 1997, *The Effect of Between Fibre Coefficient of Variation of the Fibre Fineness Measured by Airflow*

[2] A.R. Lindsay & J.W. Marler, IWTO Technology & Standards Committee, Report No. 13, May 1997, *The Importance of the Coefficient of Variation of Fibre Diameter of Blends of Wool Tops when measured by Airflow, Laserscan and OFDA.*

[3] H. Darcy, Libraire des Corps Imperiaux des Ponts et Chaussees et des Mines, 1857, *Les Fontaines Publiques de la Ville de Dijon*

[4] A. G Greenhill, Proc. London Math. Soc., **13**, 43-46, 1881, *On the Flow of Viscous Liquid in a Pipe or Channel*

[5] F. C Blake Trans. Amer. Soc. Chem. Engrs, **14**, 415-421, 1922, *The Resistance of Packing to Fluid Flow*

[6] J Kozeny, Sitzungsber. Akad. Wiss., Vienna, Abs. IIIa, **136**, 276-306, 1927, *Uber kapillare Leitung des Wassers im Boden,* Wasserkraft Wasserwirtschaft, **22**(5) , 67-70, 1927, *Uber Grundwasserbewegung*

[7] P. C. Carman, Trans. Inst. Chem. Eng., **15**, 150-166, 1937, *Fluid Flow through Granular Beds*

[8] P. C. Carman, J. Soc. Chem. Ind., **57**, 225-234, 1938, *The Determination of the Specific Surface of Powders.*

[9] E.J Wiggins, W.B. Campbell & O.J. Maas, Canadian Res., **17**(B), 318-324, 1939, *Determination of the Specific Surface of Fibrous Materials*

[10] J.L. Fowler & K.L. Hertel, J. App. Physics, **11**, 496-502, 1940, *Flow of Gas Through Porous Media*

[11] R.R Sullivan & K.L. Hertel, Text. Res., **11**, 30-38, 1940., *Surface per Gram of Cotton Fibres as a Measure of Fineness*

[12] M.A. Grimes, Text. Res. J., **13**(1), 12-18, 1942, *Measuring Fibre Fineness*

[13] A. B. D Cassie, J. Text. Inst. (Trans), 23, T195-T204, 1942, *The Porous Plug and Fibre Diameter Measurement. A Practical Method of Wool Fibre Diameter Measurement*

[14] S.L.Anderson & F. L. Warburton, J. Text. Inst. (Trans), **40**, T749-T758, 1949, *The Porous Plug and Fibre Diameter Measurement. Effect of Fibre Orientation and use of Plugs of Randomised Fibres*

[15] S.L. Anderson, J. Text. Inst., **45,** 312-316, 1954, *The Air-Flow Method of Measuring Wool Fibre Fineness*

[16] F. Monfort, Annales Textiles Belges, **54**(1-3), 58-72, 1954, *Mesure du diamètre moyendes fibres de laine: intérêt industrial du dispositif air-flow de la WIRA*

[17] IWTO Standard Test Method IWT0-8-89(E), *Method of Determining Fibre Diameter and Percentage of Medullated Fibres in Wool and Other Animal Fibres by the Projection Microscope*

[18] IWTO Standard Test Method IWT0-28-93, *Determination by the Airflow Method of the Mean Fibre Diameter of Core Samples of Raw Wool*

[19] R.K. Mann, J. Text. Inst., **61**, 190- 192, 1970, *The Calibration of Air-flow Apparatus for the Determination of the Fibre Diameter of Wool*

[20] S.L. Anderson & G.E. Settle, J. Text. Inst., **61**, 193-194, 1970, *The Calibration of Air-flow Apparatus for Fibre-diameter Measurement*

[21] S.L.Anderson, Proc. IWTO Tech. Cttee., Report 15, Paris, December 1963, *Airflow method – improvement to technique*

[22] J.F.P James, J. Text. Inst., **62**(3), 172-174, 1971, *The Calibration of Air-flow Apparatus for the Determination of the Fibre Diameter of Wool*

[23] S.L. Anderson, J. Text. Inst., **62**(3), 174-175, 1971, *The Calibration of Air-flow Apparatus for the Determination of the Fibre Diameter of Wool- Reply*

[24] B.P. Baxter, M.A. Brims &T.B. Taylor, IWTO Technology & Standards Committee, Report No. 8, Nice, December 1991 and J. Text. Inst. **83**(4), 507-526, 1992, *Description and Performance of the Optical Fibre diameter Analyser, (OFDA)*

[25] P.J. Sommerville, IWTO Technology & Standards Committee, Report No 15, Boston 1997, *Measurement of the Fineness of Superfine Wool: a comparison of Airflow, Laserscan and OFDA.*

[26] P. J. Sommerville, IWTO Technology & Standards Committee, Report No. 14, Boston, May 1997, *The Effect of Between Fibre Coefficient of Variation of the Fibre Fineness Measured by Airflow*

[27] A. R. Lindsay & J.W. Marler, IWTO Technology & Standards Committee, Report No. 13, Boston, May 1997

[28] E. Lord, Text. Res. J., **46**, T191-213, 1955, *Airflow through plugs of Textile Fibres. Part I – General Flow Relations*

[29] O. Emersleben, Physik Z., **26**, 601, 1925

[30] N. Richards, Proc. Tech .Committee of IWTO, P661-666, 1954, *The Effect of Oil and Other Changes on the Results Obtained by the Air-flow Method for Measuring Wool Fibre Diameter*

[31] T. Radhakrishnan & P. Neelakantan, Textile Research Journal, May 1990, pp 293-296

[32] P.Neelakantan & T. Radhakrishnan , Textile Research Journal, June 1990, pp 329-333

[33] P.G. Swan, *Understanding the Airflow measurement of average fibre diameter*, Unpublished communication

[34] TSI incorporated, PO Box 64394, 50 Cardigan Rd, Saint Paul, MN 55164, USA

[35] Mironer, A, *Engineering Fluid Mechanics*, McGraw-Hill International, 1979, page 24

[36] Carman, P. C. & Arnell, J. C., Canadian J. Res. , 25(A), 128-136, 1947, *Surface Area Measurements of Fine Powders Using Modified Permeability Equations*

[37] Stearn, A. E., J. Text. Inst., **62**(7), 353-360, 1971, *The Effect of Anisotropy in the Randomness of Fibre Orientation on Fibre to Fibre Contacts*

[38] J F P James & M R Bow, J. Text. Institute, **59**, 496, 1968

[39] J G Downes & R Mackie, J. Text. Institute, **60**, 547, 1969

[40] B P Baxter, Report to the IWTO Raw Wool Certification Sub-Committee, Paris, 1989, *A Simple Method of Improving Within-Laboratory Precision in the Airflow Test for Mean Fibre Diameter of Raw Wool.*

[41] R. Bowness, Personal communication to B.P. Baxter, 1989

[42] P J Sommerville, IWTO Technology & Standards Committee, Report No. CTF 04, Nice, December 1997 *Measurement of the Fineness of Superfine Wool: Effect of the Revised LASERSCAN Calibration Function of comparisons between Airflow, LASERSCAN and OFDA*